PERGAMON

International Journal of Solids and Structures 40 (2003) 777–806

INTERNATIONAL JOURNAL OF SOLIDS and STRUCTURES

www.elsevier.com/locate/ijsolstr

Analytical solutions for bending and flexure of helically reinforced cylinders

J.A. Crossley, A.J.M. Spencer, A.H. England *

Division of Theoretical Mechanics, School of Mathematical Sciences, University of Nottingham, Nottingham NG7 2RD, UK

Received 7 June 2002; received in revised form 7 October 2002

Abstract

There has been a great deal of interest in the problems of modelling cables and ropes. A recent review by Cardou and Jolicoeur [Appl. Mech. Rev. 50 (1997) 1] considers the modelling of a cable which consists of a central core surrounded by one or several helically wound wire layers. One approach has been to consider the deformations of an individual helical wire and to synthesise the model of a cable by using contact conditions between the various wires. Other authors have adopted a continuum approach regarding each layer as a transversely isotropic material whose principal direction is along a helix surrounding the central axis of the cable. In each layer the helix angle is constant so that, when referred to cylindrical polar co-ordinates, the cylinder has a constant stiffness matrix in each layer. The intention in this paper is to use the continuum approach and describe the analytical solutions that govern the simple bending, flexure, or bending under a uniform load, of an anisotropic elastic cylinder consisting of a single material of this type. The extension of this work to a composite cylinder consisting of several concentric layers, surrounding a central core, which are either bonded together or make a frictionless contact, is briefly described.

Keywords: Cable; Cylinder; Elastic; Anisotropic; Flexure

1. Introduction

There has been a great deal of interest in the problems of modelling cables and ropes. Costello (1997) describes how a strand is formed by helically winding wire around a central core. A rope or cable may be produced by helically winding several strands so that they form a cylindrical layer about a central core. A cable may have a central core and several coaxial helically wound cylindrical layers with different winding angles and strands in each layer. This produces a very complicated mechanical assembly which can deform under extension, torsion and bending and in which the contact forces between the wires and between the strands influence the behaviour of the cable. A number of different hypotheses have been put forward to model such cables. Some take into account the bending and torsional stiffness of the wires and infer the

* Corresponding author.
E-mail address: a.h.england@nottingham.ac.uk (A.H. England).

PII: S0020-7683(02)00625-X

overall behaviour of the cable by synthesis from its constituent wires or strands. This is referred to as the discrete approach. A second approach, referred to by Cardou and Jolicoeur (1997) as the semi-continuous approach, replaces each wire layer by an equivalent orthotropic elastic continuum. This is the approach which will be adopted in this paper.

The recent review by Cardou and Jolicoeur (1997) examines this field and cites 107 papers. Previous reviews by Costello (1978), Utting and Jones (1984) and Utting (1994) indicate the interest in and the importance of solutions in this field. The intention in this paper is to adopt a continuum approach and regard each layer as a transversely isotropic material whose principal direction is along a helix surrounding the central axis of the cable. In each layer the helix angle is constant so that, when referred to cylindrical polar co-ordinates, the cylinder has a constant stiffness matrix in each layer. We find exact solutions for the simple bending, flexure and bending under a uniform load of an anisotropic cylinder (sometimes referred to as a helical strand) consisting of a single material of this type. The extension of this work to a hollow cylinder or to a composite cable consisting of several concentric layers surrounding a central core is briefly described.

It may be shown that the coupled problem of the axial extension and torsion of a composite cylinder of this type separates analytically from the bending problems considered in this paper. Blouin and Cardou (1989) have solved this axial extension and torsion problem. However, although we shall concern ourselves entirely with the bending of such cylinders, it should be remembered that bending is often accompanied by axial tension and that the overall stress field will be the sum of the two linear elastic stress fields. In particular, axial extension generates an inter-layer pressure which is known to influence the bending stiffness in experiments on some composite cables. Jolicoeur and Cardou (1994) have found the analytical solution for simple bending of coaxial helically reinforced hollow cylinders of this type. The solution is found using a stress function due to Lekhnitskii (1981). Two cases are considered; either perfect bonding between the cylindrical layers, or no friction between the layers. A numerical example based on a two-layer cylinder is given. A very good agreement is found between the results obtained using the theory presented in this paper and these published results. Jolicoeur and Cardou (1996) have also made a comparison of the results they have obtained for simple bending for the semi-continuous model with results obtained by the discrete approach (see, for example, Lanteigne (1985) and the work of other authors, in particular with the long series of papers by Raoof and his co-workers, see Raoof and Kraincanic (1994)). In general good agreement is achieved between the semi-continuous model, some discrete models and some experimental results for extensional, torsional and bending stiffness.

Obviously the end conditions on these cylinders influence their behaviour in bending. The intention in this paper is to derive analytical results in a Saint-Venant sense for simple bending, flexure and bending under a uniform load for a cylinder with a traction-free surface. We assume one end of the cylinder is fixed and known resultant shear forces and bending moments are applied at the other end of the cylinder. The analytical results will hold at points in the cylinder sufficiently 'far removed' from the ends.

Section 2 formulates the problem and gives a general analysis of bending of the cylinder. Section 3 considers the simple bending of the cylinder under an applied moment over its end. Section 4 considers the flexure of the cylinder by a resultant shear force applied to its end and Section 5 considers its behaviour under a uniform transverse load in the form of a body force. Section 6 summarises the extension of this work to composite cylinders and Section 7 briefly considers a one-dimensional model for the bending of the cylinder. The paper closes with a brief discussion.

2. General analysis of bending of a cylinder

The basic constitutive equations for a transversely isotropic linearly elastic material with a preferred direction along the unit vector $\boldsymbol{a}$ have been expressed by Spencer (1984) as

$$\sigma_{ij} = \lambda e_{kk}\delta_{ij} + 2\mu_T e_{ij} + \alpha(a_k a_\ell e_{k\ell}\delta_{ij} + a_i a_j e_{kk}) + 2(\mu_L - \mu_T)(a_i a_k e_{kj} + a_j a_k e_{ki}) + \beta a_i a_j a_k a_\ell e_{k\ell}, \tag{2.1}$$

where the elastic constants λ, α, β may be expressed directly in terms of the extension moduli E_L and E_T for uniaxial tension along and orthogonal to the direction $\boldsymbol{a}$, the Poisson's ratios ν_L and ν_T associated with these extensions, and μ_L and μ_T which are the shear moduli along and orthogonal to the direction $\boldsymbol{a}$. Only five of these constants are independent. These relations are given in Appendix A.

We suppose the cylinder is helically reinforced by winding this transversely isotopic material in a helix of constant radius about the cylinder axis. We assume the helix angle $\delta(r)$ is measured relative to the cylinder axis and is a function of the radius r. Taking the z-axis along the axis of the cylinder using the unit vectors $\boldsymbol{e}_r$, $\boldsymbol{e}_\theta$ and $\boldsymbol{e}_z$ in the radial, circumferential and axial directions we find

$$\boldsymbol{a} = \sin\delta(r)\boldsymbol{e}_\theta + \cos\delta(r)\boldsymbol{e}_z. \tag{2.2}$$

The stress–strain relations (2.1) can then be transformed into the cylindrical polar co-ordinate system

$$\begin{pmatrix} \sigma_{rr} \\ \sigma_{\theta\theta} \\ \sigma_{zz} \\ \sigma_{\theta z} \\ \sigma_{rz} \\ \sigma_{r\theta} \end{pmatrix} = \begin{pmatrix} c_{11} & c_{12} & c_{13} & c_{14} & 0 & 0 \\ c_{12} & c_{22} & c_{23} & c_{24} & 0 & 0 \\ c_{13} & c_{23} & c_{33} & c_{34} & 0 & 0 \\ c_{14} & c_{24} & c_{34} & c_{44} & 0 & 0 \\ 0 & 0 & 0 & 0 & c_{55} & c_{56} \\ 0 & 0 & 0 & 0 & c_{56} & c_{66} \end{pmatrix} \begin{pmatrix} e_{rr} \\ e_{\theta\theta} \\ e_{zz} \\ 2e_{\theta z} \\ 2e_{rz} \\ 2e_{r\theta} \end{pmatrix}, \tag{2.3}$$

where the 13 elastic stiffnesses are related to the moduli E_L, E_T, μ_L, μ_T, ν_L, ν_T and the helix angle $\delta(r)$ (see Appendix A). This gives the stress–strain relation at a point on the cylindrical surface $r =$ constant. If the lay-angle δ is constant then (2.3) is the stress–strain relation at all points of the cylinder and the stiffnesses c_{ij} are constant. In the case of a composite cylinder such as a cable or wire rope which is produced by winding several different layers to form the cylinder, we can suppose the elastic constants and the lay angle are piecewise functions of r and divide the cylinder into cylindrical shells in each of which the stiffnesses are constant. This is referred to by Blouin and Cardou (1989) as the semi-continuous model of a stranded wire.

In this section we examine a solid cylinder in which the elastic constants in (2.3) are constant. Composite cylinders are considered in Section 6.

In cylindrical polar co-ordinates the equations of equilibrium are

$$\begin{aligned} &\frac{\partial\sigma_{rr}}{\partial r} + \frac{1}{r}\frac{\partial\sigma_{r\theta}}{\partial\theta} + \frac{\partial\sigma_{rz}}{\partial z} + \frac{\sigma_{rr} - \sigma_{\theta\theta}}{r} + \boldsymbol{F}\cdot\boldsymbol{e}_r = 0, \\ &\frac{\partial\sigma_{r\theta}}{\partial r} + \frac{1}{r}\frac{\partial\sigma_{\theta\theta}}{\partial\theta} + \frac{\partial\sigma_{\theta z}}{\partial z} + \frac{2\sigma_{r\theta}}{r} + \boldsymbol{F}\cdot\boldsymbol{e}_\theta = 0, \\ &\frac{\partial\sigma_{rz}}{\partial r} + \frac{1}{r}\frac{\partial\sigma_{\theta z}}{\partial\theta} + \frac{\partial\sigma_{zz}}{\partial z} + \frac{\sigma_{rz}}{r} + \boldsymbol{F}\cdot\boldsymbol{e}_z = 0, \end{aligned} \tag{2.4}$$

where $\boldsymbol{F}$ is the body force per unit volume and the strain–displacement relations are

$$\begin{aligned} &e_{rr} = \frac{\partial u_r}{\partial r}, \quad e_{\theta\theta} = \frac{1}{r}\frac{\partial u_\theta}{\partial\theta} + \frac{u_r}{r}, \quad e_{zz} = \frac{\partial u_z}{\partial z}, \quad e_{\theta z} = \frac{1}{2}\left(\frac{\partial u_\theta}{\partial z} + \frac{1}{r}\frac{\partial u_z}{\partial\theta}\right), \\ &e_{rz} = \frac{1}{2}\left(\frac{\partial u_r}{\partial z} + \frac{\partial u_z}{\partial r}\right), \quad e_{r\theta} = \frac{1}{2}\left(\frac{1}{r}\frac{\partial u_r}{\partial\theta} + \frac{\partial u_\theta}{\partial r} - \frac{1}{r}u_\theta\right), \end{aligned} \tag{2.5}$$

where the displacement field is $\boldsymbol{u} = u_r\boldsymbol{e}_r + u_\theta\boldsymbol{e}_\theta + u_z\boldsymbol{e}_z$.

We look for solutions in which the axis ($r = 0$) of the cylinder is bent in the (x, z) plane into a parabolic, cubic or fourth-order curve of the form $(1/2)Cz^2 + (1/6)Dz^3 + (1/24)Ez^4$ in which C, D and E are known constants. We assume the displacement field has the form

$$\begin{aligned}
u_r &= \left(F_1 r^q + F_3 z r^{q-1} + \frac{1}{2}F_5 z^2 r^{q-2} + \frac{1}{2}Cz^2 + \frac{1}{6}Dz^3 + \frac{1}{24}Ez^4\right)\cos\theta + (F_2 r^q + F_4 z r^{q-1})\sin\theta,\\
u_\theta &= \left(G_1 r^q + G_3 z r^{q-1} + \frac{1}{2}G_5 z^2 r^{q-2} - \frac{1}{2}Cz^2 - \frac{1}{6}Dz^3 - \frac{1}{24}Ez^4\right)\sin\theta + (G_2 r^q + G_4 z r^{q-1})\cos\theta,\\
u_z &= \left(H_1 r^q + H_3 z r^{q-1} + \frac{1}{2}H_5 z^2 r^{q-2}\right)\sin\theta + \left(H_2 r^q + H_4 z r^{q-1} - Crz - \frac{1}{2}Drz^2 - \frac{1}{6}Erz^3\right)\cos\theta,
\end{aligned} \tag{2.6}$$

in which the exponent q is a constant and the 15 constants $F_1, \dots, H_5$ are to be determined from the equilibrium equations and the boundary conditions. It is convenient to express these constants in the column vector form

$$\boldsymbol{Z} = (F_1, G_1, H_1, F_2, G_2, H_2, \dots, F_5, G_5, H_5)^{\mathrm{T}}. \tag{2.7}$$

If the strains (2.5) are calculated from the displacement field (2.6), and the stress field formed from (2.3), then the stresses may be substituted into the equilibrium equations (2.4) to form the equivalent of Navier's displacement equations of equilibrium.

These equilibrium equations must hold for all values of θ, z and r. It may be shown that they reduce to the following system of 15 equations for the 15 unknowns in $\boldsymbol{Z}$

$$\boldsymbol{M}(q)\boldsymbol{Z} = \boldsymbol{R}, \tag{2.8}$$

where the right-hand side vector has the following form

$$\boldsymbol{R} = Cr^{(2-q)}\boldsymbol{R}_1 + W_0 r^{(2-q)}\boldsymbol{R}_2 + Dr^{(3-q)}\boldsymbol{R}_3 + Er^{(4-q)}\boldsymbol{R}_4, \tag{2.9}$$

where

$$\begin{aligned}
\boldsymbol{R}_1 &= (2c_{13} - c_{23}, -c_{23}, -c_{34}, 0, \dots, 0)^{\mathrm{T}},\\
\boldsymbol{R}_2 &= (-1, 1, 0, \dots, 0)^{\mathrm{T}},\\
\boldsymbol{R}_3 &= (0, 0, 0, 0, c_{34}, c_{33}, 2c_{13} - c_{23}, -c_{23}, -c_{34}, 0, \dots, 0)^{\mathrm{T}},\\
\boldsymbol{R}_4 &= (0, \dots, 0, c_{34}, c_{33}, 2c_{13} - c_{23}, -c_{23}, -c_{34})^{\mathrm{T}}.
\end{aligned} \tag{2.10}$$

In the system of equations (2.8) it should be noted that the simple-bending constant C only enters the first three equations, the flexure constant D only enters equations 5 to 9 and the fourth-order bending constant E only enters equations 11 to 15. We have inserted a constant body force $\boldsymbol{F} = W_0\boldsymbol{i}$ (parallel to the $\theta = 0$ direction) into the equilibrium equations and this only enters the first and second equations of the system (2.8).

The 15×15 matrix $\boldsymbol{M}(q)$ on the left-hand side of (2.8) is a constant matrix whose coefficients depend on the exponent q. It may be partitioned into a set of 3×3 matrices, as shown in (2.11):

$$\boldsymbol{M}(q) = \begin{pmatrix}
\boldsymbol{M}_{11}(q) & \boldsymbol{0} & \boldsymbol{0} & \boldsymbol{M}_{14}(q) & \boldsymbol{M}_{15}(q)\\
\boldsymbol{0} & \boldsymbol{M}_{22}(q) & \boldsymbol{M}_{23}(q) & \boldsymbol{0} & \boldsymbol{0}\\
\boldsymbol{0} & \boldsymbol{0} & \boldsymbol{M}_{33}(q) & \boldsymbol{0} & \boldsymbol{0}\\
\boldsymbol{0} & \boldsymbol{0} & \boldsymbol{0} & \boldsymbol{M}_{44}(q) & \boldsymbol{M}_{45}(q)\\
\boldsymbol{0} & \boldsymbol{0} & \boldsymbol{0} & \boldsymbol{0} & \boldsymbol{M}_{55}(q)
\end{pmatrix}. \tag{2.11}$$

These submatrices are detailed in Appendix B. The matrices on the leading diagonal are closely related to each other. Matrices $\boldsymbol{M}_{11}(q)$ and $\boldsymbol{M}_{22}(q)$ have the same characteristic equation corresponding to $\det \boldsymbol{M}_{11}(q) = 0$, $\det \boldsymbol{M}_{22}(q) = 0$ and the same set of roots which we will refer to as the eigenvalues.

We can also observe that

$$\begin{aligned} \boldsymbol{M}_{33}(q) &= \boldsymbol{M}_{11}(q-1), \quad \boldsymbol{M}_{44}(q) = \boldsymbol{M}_{22}(q-1), \\ \boldsymbol{M}_{55}(q) &= \boldsymbol{M}_{11}(q-2), \quad \boldsymbol{M}_{45}(q) = \boldsymbol{M}_{23}(q-1). \end{aligned} \tag{2.12}$$

Hence the eigenvalues of the system are closely related to the eigenvalues of $\boldsymbol{M}_{11}(q)$. Expansion of the determinant of the 3×3 matrix $\boldsymbol{M}_{11}(q)$ yields a cubic in q^2 of the form

$$\det \boldsymbol{M}_{11}(q) = q^2(\alpha q^4 + \beta q^2 + \gamma) = 0. \tag{2.13}$$

The constants α, β and γ are cubic terms in the c_{ij}. There are six eigenvalues $q = q_i$ which we denote by $q = q_1 = 0$, $q = q_2$, $q = q_3$, $q_4 = -q_2$, $q_5 = -q_3$ and we will cope separately with the double root at the origin in due course. The non-negative roots q_1, q_2, q_3 correspond to displacements which are finite or zero along the axis $r = 0$ of the cylinder. The negative roots and the second solution corresponding to the double root at $q = 0$ give rise to solutions which are singular on $r = 0$. The numerical examples considered to date have not given rise to complex roots.

The solution of the system (2.8) consists of four particular solutions corresponding to the terms (2.9) on the right-hand side of (2.8) together with the eigenvector solutions. The particular solutions are found by putting $q = 2$ or 3 or 4 in (2.8) and solving the resulting partitioned system (assuming 2, 3 or 4 are not eigenvalues).

For simple bending, the particular solution is

$$C\boldsymbol{Z}_C = C(\boldsymbol{Z}_{C1}^{\mathrm{T}}, 0, \ldots, 0)^{\mathrm{T}}, \tag{2.14}$$

where $\boldsymbol{Z}_{C1}$ is the 3×1 vector given by

$$\boldsymbol{Z}_{C1} = \boldsymbol{M}_{11}^{-1}(2)\boldsymbol{R}_{10}, \quad \boldsymbol{R}_{10} = (2c_{13} - c_{23}, -c_{23}, -c_{34})^{\mathrm{T}}. \tag{2.15}$$

For a body force, the particular solution is

$$W_0\boldsymbol{Z}_W = W_0\big(\boldsymbol{Z}_{W1}^{\mathrm{T}}, 0, \ldots, 0\big)^{\mathrm{T}}, \tag{2.16}$$

where

$$\boldsymbol{Z}_{W1} = \boldsymbol{M}_{11}^{-1}(2)\boldsymbol{R}_{11}, \quad \boldsymbol{R}_{11} = (-1, 1, 0)^{\mathrm{T}}. \tag{2.17}$$

For flexure, the particular solution is

$$D\boldsymbol{Z}_D = D\big(0, 0, 0, \boldsymbol{Z}_{D2}^{\mathrm{T}}, \boldsymbol{Z}_{D3}^{\mathrm{T}}, 0, \ldots, 0\big)^{\mathrm{T}}, \tag{2.18}$$

where

$$\boldsymbol{Z}_{D3} = \boldsymbol{M}_{33}^{-1}(3)\boldsymbol{R}_{33}, \quad \text{where } \boldsymbol{R}_{33} = \boldsymbol{R}_{10}, \tag{2.19}$$

$$\boldsymbol{Z}_{D2} = \boldsymbol{M}_{22}^{-1}(3)[\boldsymbol{R}_{32} - \boldsymbol{M}_{23}(3)\boldsymbol{Z}_{D3}], \tag{2.20}$$

$$\boldsymbol{R}_{32} = (0, c_{34}, c_{33})^{\mathrm{T}}. \tag{2.21}$$

Note also that $\boldsymbol{M}_{33}(3) = \boldsymbol{M}_{11}(2)$ so that

$$\boldsymbol{Z}_{D3} = \boldsymbol{Z}_{C1}. \tag{2.22}$$

The fourth-order particular solution is found by putting $q = 4$ and has the form

$$E\boldsymbol{Z}_E = E\big(\boldsymbol{Z}_{E1}^{\mathrm{T}}, \boldsymbol{0}, \boldsymbol{0}, \boldsymbol{Z}_{E4}^{\mathrm{T}}, \boldsymbol{Z}_{E5}^{\mathrm{T}}\big)^{\mathrm{T}}, \tag{2.23}$$

where

$$\boldsymbol{Z}_{E5} = \boldsymbol{M}_{55}^{-1}(4)\boldsymbol{R}_{10}, \tag{2.24}$$

$$\boldsymbol{Z}_{E4} = \boldsymbol{M}_{44}^{-1}(4)[\boldsymbol{R}_{32} - \boldsymbol{M}_{45}(4)\boldsymbol{Z}_{E5}], \tag{2.25}$$

$$\boldsymbol{Z}_{E1} = -\boldsymbol{M}_{11}^{-1}(4)[\boldsymbol{M}_{14}(4)\boldsymbol{Z}_{E4} + \boldsymbol{M}_{15}(4)\boldsymbol{Z}_{E5}], \tag{2.26}$$

but, if we observe that $\boldsymbol{M}_{55}(4) = \boldsymbol{M}_{11}(2)$ and $\boldsymbol{M}_{44}(4) = \boldsymbol{M}_{22}(3)$ and $\boldsymbol{M}_{45}(4) = \boldsymbol{M}_{23}(3)$, we see that

$$\boldsymbol{Z}_{E5} = \boldsymbol{Z}_{C1} \quad \text{and} \quad \boldsymbol{Z}_{E4} = \boldsymbol{Z}_{D2}, \tag{2.27}$$

so that there are close relations between the particular solutions (2.14), (2.16), (2.18) and (2.23).

The eigenvector solutions satisfy the system of linear equations

$$\begin{pmatrix} \boldsymbol{M}_{11}(q) & \boldsymbol{0} & \boldsymbol{0} & \boldsymbol{M}_{14}(q) & \boldsymbol{M}_{15}(q) \\ \boldsymbol{0} & \boldsymbol{M}_{22}(q) & \boldsymbol{M}_{23}(q) & \boldsymbol{0} & \boldsymbol{0} \\ \boldsymbol{0} & \boldsymbol{0} & \boldsymbol{M}_{33}(q) & \boldsymbol{0} & \boldsymbol{0} \\ \boldsymbol{0} & \boldsymbol{0} & \boldsymbol{0} & \boldsymbol{M}_{44}(q) & \boldsymbol{M}_{45}(q) \\ \boldsymbol{0} & \boldsymbol{0} & \boldsymbol{0} & \boldsymbol{0} & \boldsymbol{M}_{55}(q) \end{pmatrix} \begin{pmatrix} \boldsymbol{Z}_1 \\ \boldsymbol{Z}_2 \\ \boldsymbol{Z}_3 \\ \boldsymbol{Z}_4 \\ \boldsymbol{Z}_5 \end{pmatrix} = \boldsymbol{0}, \tag{2.28}$$

which may be partitioned into the 3×3 and 3×1 matrices as shown.

Because $\boldsymbol{M}_{11}(q)$ and $\boldsymbol{M}_{22}(q)$ have the same characteristic equation, and the other matrices on the leading diagonal are related to these matrices by (2.12), we can express all of the eigenvectors in terms of the eigenvalues $q = q_i$, $i = 1, \ldots, 5$. In this section we are concerned with solutions which are well behaved as $r \to 0$, so we will restrict consideration to the non-negative eigenvalues $q_1 = 0$, q_2 and q_3 of $\det \boldsymbol{M}_{11}(q) = 0$. We denote the eigenvector corresponding to the eigenvalue $q = e_i$ of $\boldsymbol{M}(q)$ by $\boldsymbol{E}_i = (\boldsymbol{Z}_1^{(i)\mathrm{T}}, \boldsymbol{Z}_2^{(i)\mathrm{T}}, \ldots, \boldsymbol{Z}_5^{(i)\mathrm{T}})^{\mathrm{T}}$ for $i = 1, \ldots, 15$.

$$\textbf{Eigenvalue } e_1 = q_1 = 0, \quad \boldsymbol{M}_{11}(0)\boldsymbol{Z}_1^{(1)} = \boldsymbol{0}. \tag{2.29}$$

Examination of this equation shows

$$\boldsymbol{Z}_1^{(1)} = (1, -1, 0)^{\mathrm{T}}. \tag{2.30}$$

Hence the first eigenvector is

$$\boldsymbol{E}_1 = (\boldsymbol{Z}_1^{(1)\mathrm{T}}, \boldsymbol{0}, \boldsymbol{0}, \boldsymbol{0}, \boldsymbol{0})^{\mathrm{T}}, \tag{2.31}$$

$$\textbf{Eigenvalue } e_2 = q_2, \quad \boldsymbol{M}_{11}(q_2)\boldsymbol{Z}_1^{(2)} = \boldsymbol{0}. \tag{2.32}$$

If we take the first component of $\boldsymbol{Z}_1^{(2)}$ as unity so $\boldsymbol{Z}_1^{(2)} = (1, v_2, v_3)^{\mathrm{T}}$ then v_2 and v_3 satisfy the equations

$$\begin{pmatrix} c_{66}q_2^2 - c_{22} - c_{66} & c_{56}(q_2^2 + q_2) - c_{24} \\ c_{56}(q_2^2 - q_2) - c_{24} & c_{55}q_2^2 - c_{44} \end{pmatrix} \begin{pmatrix} v_2 \\ v_3 \end{pmatrix} = \begin{pmatrix} (c_{12} + c_{66})q_2 + c_{22} + c_{66} \\ (c_{56} + c_{14})q_2 + c_{24} \end{pmatrix}. \tag{2.33}$$

This can be written as a 2×2 system

$$\boldsymbol{N}(q_2)\boldsymbol{V}_2(q_2) = \boldsymbol{S}(q_2), \tag{2.34}$$

where $\boldsymbol{V}_2(q_2) = (v_2, v_3)^{\mathrm{T}}$ and $\boldsymbol{N}(q_2)$ and $\boldsymbol{S}(q_2)$ are the remaining matrices in (2.23). Hence the eigenvector corresponding to $q = q_2$ is

$$\boldsymbol{E}_2 = \left(\boldsymbol{Z}_1^{(2)\mathrm{T}}, \boldsymbol{0}, \boldsymbol{0}, \boldsymbol{0}, \boldsymbol{0}\right)^{\mathrm{T}}, \tag{2.35}$$

where

$$\boldsymbol{Z}_1^{(2)} = \left(1, \boldsymbol{V}_2^{\mathrm{T}}(q_2)\right)^{\mathrm{T}}, \tag{2.36}$$

and the column vector $\boldsymbol{V}_2$ satisfies (2.34).

Eigenvalue $e_3 = q_3, \quad \boldsymbol{M}_{11}(q_3)\boldsymbol{Z}_1^{(3)} = \boldsymbol{0}.$

Similarly the eigenvector is given by

$$\boldsymbol{E}_3 = (\boldsymbol{Z}_1^{(3)\mathrm{T}}, \boldsymbol{0}, \boldsymbol{0}, \boldsymbol{0}, \boldsymbol{0})^{\mathrm{T}}, \tag{2.37}$$

where

$$\boldsymbol{Z}_1^{(3)} = (1, \boldsymbol{V}_2^{\mathrm{T}}(q_3))^{\mathrm{T}}, \tag{2.38}$$

and $\boldsymbol{V}_2(q_3)$ satisfies (2.34) with q_2 replaced by q_3.

The matrix $\boldsymbol{M}_{22}(q)$ is very closely related to the matrix $\boldsymbol{M}_{11}(q)$ and has the same eigenvalues. The eigenvectors corresponding to $\boldsymbol{M}_{22}(q)$ satisfy the system $\boldsymbol{M}_{22}(q)\ \boldsymbol{Z}_2 = \boldsymbol{0}$ and are easily shown to be

$$\begin{aligned}
&\textbf{Eigenvalue}\ e_4 = q_1 = 0, \quad && \boldsymbol{E}_4 = (\boldsymbol{0}, \boldsymbol{Z}_2^{(4)\mathrm{T}}, \boldsymbol{0}, \boldsymbol{0}, \boldsymbol{0})^{\mathrm{T}},\\
&\textbf{Eigenvalue}\ e_5 = q_2, && \boldsymbol{E}_5 = (\boldsymbol{0}, \boldsymbol{Z}_2^{(5)\mathrm{T}}, \boldsymbol{0}, \boldsymbol{0}, \boldsymbol{0})^{\mathrm{T}},\\
&\textbf{Eigenvalue}\ e_6 = q_3, && \boldsymbol{E}_6 = (\boldsymbol{0}, \boldsymbol{Z}_2^{(6)\mathrm{T}}, \boldsymbol{0}, \boldsymbol{0}, \boldsymbol{0})^{\mathrm{T}},
\end{aligned} \tag{2.39}$$

where the second and third components of $\boldsymbol{Z}_2^{(5)}$ and $\boldsymbol{Z}_2^{(6)}$ satisfy Eq. (2.34) with the sign of the right-hand side reversed, so that

$$\boldsymbol{Z}_2^{(4)} = (1,1,0)^{\mathrm{T}}, \boldsymbol{Z}_2^{(5)} = (1, -\boldsymbol{V}_2^{\mathrm{T}}(q_2))^{\mathrm{T}} \quad \text{and} \quad \boldsymbol{Z}_2^{(6)} = (1, -\boldsymbol{V}_2^{\mathrm{T}}(q_3))^{\mathrm{T}}. \tag{2.40}$$

The eigenvectors corresponding to the matrix $\boldsymbol{M}_{33}(q)$ satisfy the system

$$\boldsymbol{M}_{33}(q)\boldsymbol{Z}_3 = 0, \qquad \boldsymbol{M}_{22}(q)\boldsymbol{Z}_2 = -\boldsymbol{M}_{23}(q)\boldsymbol{Z}_3. \tag{2.41}$$

Since $\boldsymbol{M}_{33}(q) = \boldsymbol{M}_{11}(q-1)$, the eigenvalues of $\boldsymbol{M}_{33}$ are $q = 1 + q_1,\ 1 + q_2$ and $1 + q_3$. Consequently $\boldsymbol{Z}_3$ satisfies the system $\boldsymbol{M}_{11}(q_i)\boldsymbol{Z}_3 = \boldsymbol{0}$ and hence the $\boldsymbol{Z}_3$ components of the eigenvectors are identical to those of $\boldsymbol{M}_{11}$. Hence when $q = 1 + q_i$ the eigenvectors have the components

$$\boldsymbol{Z}_3^{(6+i)} = \boldsymbol{Z}_1^{(i)},\ \ i = 1,2,3 \quad \text{and} \quad \boldsymbol{Z}_2^{(6+i)} = -\boldsymbol{M}_{22}^{-1}(1+q_i)\boldsymbol{M}_{23}(1+q_i)\boldsymbol{Z}_1^{(i)},\ \ i = 1,2,3, \tag{2.42}$$

$$\begin{aligned}
&\textbf{Eigenvalue}\ e_7 = 1 + q_1, \quad \boldsymbol{E}_7 = (\boldsymbol{0}, -\{\boldsymbol{M}_{22}^{-1}(1+q_1)\boldsymbol{M}_{23}(1+q_1)\boldsymbol{Z}_1^{(1)}\}^{\mathrm{T}}, \boldsymbol{Z}_1^{(1)\mathrm{T}}, \boldsymbol{0}, \boldsymbol{0})^{\mathrm{T}},\\
&\textbf{Eigenvalue}\ e_8 = 1 + q_2, \quad \boldsymbol{E}_8 = (\boldsymbol{0}, -\{\boldsymbol{M}_{22}^{-1}(1+q_2)\boldsymbol{M}_{23}(1+q_2)\boldsymbol{Z}_1^{(2)}\}^{\mathrm{T}}, \boldsymbol{Z}_1^{(2)\mathrm{T}}, \boldsymbol{0}, \boldsymbol{0})^{\mathrm{T}},\\
&\textbf{Eigenvalue}\ e_9 = 1 + q_3, \quad \boldsymbol{E}_9 = (\boldsymbol{0}, -\{\boldsymbol{M}_{22}^{-1}(1+q_3)\boldsymbol{M}_{23}(1+q_3)\boldsymbol{Z}_1^{(3)}\}^{\mathrm{T}}, \boldsymbol{Z}_1^{(3)\mathrm{T}}, \boldsymbol{0}, \boldsymbol{0})^{\mathrm{T}}.
\end{aligned} \tag{2.43}$$

Matrix manipulation easily shows that $\boldsymbol{Z}_2^{(7)} = (0,0,-1)^{\mathrm{T}}$.

Since the matrix $\boldsymbol{M}_{44}(q)$ is equal to $\boldsymbol{M}_{22}(q-1)$ it also has the eigenvalues $q = 1 + q_i$. The eigenvectors satisfy the equations

$$\boldsymbol{M}_{44}(q)\boldsymbol{Z}_4 = \boldsymbol{0}, \qquad \boldsymbol{M}_{11}(q)\boldsymbol{Z}_1 = -\boldsymbol{M}_{14}\boldsymbol{Z}_4. \tag{2.44}$$

Hence component $\boldsymbol{Z}_4$ of the eigenvector, corresponding to the eigenvalue $1 + q_i$, satisfies the equation $\boldsymbol{M}_{22}(q_i)\boldsymbol{Z}_4 = \boldsymbol{0}$, so that the eigenvector components $\boldsymbol{Z}_4^{(i+6)}$ are identical to $\boldsymbol{Z}_2^{(i)}$ defined in (2.40). The corresponding values of $\boldsymbol{Z}_1$ are $-\boldsymbol{M}_{11}^{-1}(1+q_i)\boldsymbol{M}_{14}(1+q_i)\boldsymbol{Z}_2^{(i)}$. Hence

$$\begin{aligned}
&\textbf{Eigenvalue}\ e_{10} = 1 + q_1, \quad \boldsymbol{E}_{10} = (-\{\boldsymbol{M}_{11}^{-1}(1+q_1)\boldsymbol{M}_{14}(1+q_1)\boldsymbol{Z}_2^{(4)}\}^{\mathrm{T}}, \boldsymbol{0}, \boldsymbol{0}, \boldsymbol{Z}_2^{(4)\mathrm{T}}, \boldsymbol{0})^{\mathrm{T}},\\
&\textbf{Eigenvalue}\ e_{11} = 1 + q_2, \quad \boldsymbol{E}_{11} = (-\{\boldsymbol{M}_{11}^{-1}(1+q_2)\boldsymbol{M}_{14}(1+q_2)\boldsymbol{Z}_2^{(5)}\}^{\mathrm{T}}, \boldsymbol{0}, \boldsymbol{0}, \boldsymbol{Z}_2^{(5)\mathrm{T}}, \boldsymbol{0})^{\mathrm{T}},\\
&\textbf{Eigenvalue}\ e_{12} = 1 + q_3, \quad \boldsymbol{E}_{12} = (-\{\boldsymbol{M}_{11}^{-1}(1+q_3)\boldsymbol{M}_{14}(1+q_3)\boldsymbol{Z}_2^{(6)}\}^{\mathrm{T}}, \boldsymbol{0}, \boldsymbol{0}, \boldsymbol{Z}_2^{(6)\mathrm{T}}, \boldsymbol{0})^{\mathrm{T}}.
\end{aligned} \tag{2.45}$$

Again, we can show that $\boldsymbol{Z}_1^{(10)} = (0,0,-1)^{\mathrm{T}}$.

Finally, since $\boldsymbol{M}_{55}(q) = \boldsymbol{M}_{11}(q-2)$, the eigenvalues of $\boldsymbol{M}_{55}$ are $q = 2 + q_i$. The components of the eigenvector satisfy the system

$$\begin{aligned}&\boldsymbol{M}_{55}(q)\boldsymbol{Z}_5=\mathbf{0},\\&\boldsymbol{M}_{44}(q)\boldsymbol{Z}_4=-\boldsymbol{M}_{45}(q)\boldsymbol{Z}_5,\\&\boldsymbol{M}_{11}(q)\boldsymbol{Z}_1=-\boldsymbol{M}_{14}(q)\boldsymbol{Z}_4-\boldsymbol{M}_{15}(q)\boldsymbol{Z}_5,\end{aligned}\tag{2.46}$$

but at $q=2+q_i$, $\boldsymbol{M}_{55}(q)=\boldsymbol{M}_{11}(q_i)$ and $\boldsymbol{M}_{44}(q)=\boldsymbol{M}_{22}(1+q_i)$, $\boldsymbol{M}_{45}(q)=\boldsymbol{M}_{23}(1+q_i)$, hence the first two sets of equations are identical to those of (2.41), so that $\boldsymbol{Z}_5^{(12+i)}=\boldsymbol{Z}_5^{(6+i)}=\boldsymbol{Z}_1^{(i)}$, $\boldsymbol{Z}_4^{(12+i)}=\boldsymbol{Z}_2^{(6+i)}$ for $i=1,2,3$ as defined in (2.42). Consequently, for $i=1$, 2 and 3,

$$\boldsymbol{Z}_1^{(12+i)}=-\boldsymbol{M}_{11}^{-1}(2+q_i)\left[\boldsymbol{M}_{14}(2+q_i)\boldsymbol{Z}_2^{(6+i)}+\boldsymbol{M}_{15}(2+q_i)\boldsymbol{Z}_1^{(i)}\right],\tag{2.47}$$

$$\begin{aligned}&\textbf{Eigenvalue}\ \ e_{13}=2+q_1,\quad \boldsymbol{E}_{13}=(\boldsymbol{Z}_1^{(13)\mathrm{T}},\mathbf{0},\mathbf{0},\boldsymbol{Z}_2^{(7)\mathrm{T}},\boldsymbol{Z}_1^{(1)\mathrm{T}})^{\mathrm{T}},\\&\textbf{Eigenvalue}\ \ e_{14}=2+q_2,\quad \boldsymbol{E}_{14}=(\boldsymbol{Z}_1^{(14)\mathrm{T}},\mathbf{0},\mathbf{0},\boldsymbol{Z}_2^{(8)\mathrm{T}},\boldsymbol{Z}_1^{(2)\mathrm{T}})^{\mathrm{T}},\\&\textbf{Eigenvalue}\ \ e_{15}=2+q_3,\quad \boldsymbol{E}_{15}=(\boldsymbol{Z}_1^{(15)\mathrm{T}},\mathbf{0},\mathbf{0},\boldsymbol{Z}_2^{(9)\mathrm{T}},\boldsymbol{Z}_1^{(3)\mathrm{T}})^{\mathrm{T}},\end{aligned}\tag{2.48}$$

where $\boldsymbol{Z}_1^{(12+i)}$, $\boldsymbol{Z}_2^{(6+i)}$, $\boldsymbol{Z}_1^{(i)}$ are defined by (2.47), (2.42), (2.30), (2.36) and (2.38) respectively.

A second set of eigenvectors, which correspond to solutions which are singular on $r=0$, may be found by replacing q_2 by $-q_2$ and q_3 by $-q_3$ in the above system. For completeness, additional solutions corresponding to the double root at $q=0$ should also be added to the set of eigenvectors. These have been found (see Crossley, 2002), but do not enter the solutions considered in this paper as they are singular on $r=0$. A solution of the system of equations (2.28), by the process of back substitution, will confirm that we have obtained all of the eigenvectors of the system.

Each eigenvector corresponds to a solution of the equilibrium equations in which the displacement field is given by (2.6) with $q=e_i$ and $(F_1,\dots,H_5)^{\mathrm{T}}=\boldsymbol{E}_i$ for $i=1,\dots,15$.

2.1. The eigenvector solutions

1. The solutions corresponding to the eigenvalue $q_1=0$ are the following:
   - Solution 1 $u_r=\cos\theta$, $u_\theta=-\sin\theta$, $u_z=0$, which corresponds to a rigid-body translation along the x-axis.
   - Solution 4 $u_r=\sin\theta$, $u_\theta=-\cos\theta$, $u_z=0$, which corresponds to a rigid-body translation along the y-axis.
   - Solution 7 $u_r=z\cos\theta$, $u_\theta=-z\sin\theta$, $u_z=-r\cos\theta$, which corresponds to a rigid-body rotation about the y-axis with $u_x=z$, $u_y=0$, $u_z=-x$.
   - Solution 10 $u_r=z\sin\theta$, $u_\theta=z\cos\theta$, $u_z=-r\sin\theta$, which corresponds to a rigid-body rotation about the x-axis with $u_x=0$, $u_y=z$, $u_z=-y$.
   - Solution 13 $u_r=(\frac{1}{2}z^2+\boldsymbol{Z}_1^{(13)}(1)r^2)\cos\theta$, $u_\theta=(-\frac{1}{2}z^2+\boldsymbol{Z}_1^{(13)}(2)r^2)\sin\theta$, $u_z=-zr\cos\theta+\boldsymbol{Z}_1^{(13)}(3)r^2\sin\theta$ where $\boldsymbol{Z}_1^{(13)}$ has the components $\boldsymbol{Z}_1^{(13)}(1),\boldsymbol{Z}_1^{(13)}(2),\boldsymbol{Z}_1^{(13)}(3)$. Only Solution 13 corresponds to a non-zero stress field. This is part of the simple-bending solution found in the next section.
2. Solutions corresponding to the eigenvalue $q=q_2$ are
   - Solution 2 Since $\boldsymbol{Z}_1^{(2)}=(1,v_2,v_3)^{\mathrm{T}}$ and the vector $\boldsymbol{V}_2(q_2)=(v_2,v_3)^{\mathrm{T}}$ satisfies (2.34), then $u_r=r^{q_2}\cos\theta$, $u_\theta=v_2r^{q_2}\sin\theta$, $u_z=v_3r^{q_2}\sin\theta$. This solution has a non-zero stress field.
   - Solution 5 $u_r=r^{q_2}\sin\theta$, $u_\theta=-v_2r^{q_2}\cos\theta$, $u_z=-v_3r^{q_2}\cos\theta$. This is the same solution as Solution 2 rotated through 90°.
   - Solution 8 $u_r=zr^{q_2}\cos\theta+\boldsymbol{Z}_2^{(8)}(1)r^{(q_2+1)}\sin\theta$, $u_\theta=v_2zr^{q_2}\sin\theta+\boldsymbol{Z}_2^{(8)}(2)r^{(q_2+1)}\cos\theta$, $u_z=v_3zr^{q_2}\sin\theta+\boldsymbol{Z}_2^{(8)}(3)r^{(q_2+1)}\cos\theta$ where $\boldsymbol{Z}_2^{(8)}$ has the components $\boldsymbol{Z}_2^{(8)}(1),\boldsymbol{Z}_2^{(8)}(2),\boldsymbol{Z}_2^{(8)}(3)$. The solution has a non-zero stress field.

Solution 11 Is the same solution as Solution 8 rotated through 90°.
Solution 14

$$u_r = \left(\boldsymbol{Z}_1^{(14)}(1)r^{2+q_2} + \frac{1}{2}z^2 r^{q_2}\right)\cos\theta + \boldsymbol{Z}_4^{(14)}(1)zr^{1+q_2}\sin\theta,$$
$$u_\theta = \left(\boldsymbol{Z}_1^{(14)}(2)r^{2+q_2} + v_2\frac{1}{2}z^2 r^{q_2}\right)\sin\theta + \boldsymbol{Z}_4^{(14)}(2)zr^{1+q_2}\cos\theta,$$
$$u_z = \left(\boldsymbol{Z}_1^{(14)}(3)r^{2+q_2} + v_3\frac{1}{2}z^2 r^{q_2}\right)\sin\theta + \boldsymbol{Z}_4^{(14)}(3)zr^{1+q_2}\cos\theta.$$

This solution has a non-zero stress field.

3. A similar set of solutions is produced from the eigenvalue q_3.

The complete set of solutions of the type (2.6) may be constructed by taking the sum of the particular solutions corresponding to (2.14), (2.16), (2.18), (2.23) and adding to this the solution corresponding to each eigenvector $\boldsymbol{E}_i$ multiplied by an arbitrary constant X_i, for $i = 1, \dots, 15$. Hence

$$u_r = \left(\frac{1}{2}Cz^2 + \frac{1}{6}Dz^3 + \frac{1}{24}Ez^4\right)\cos\theta + \sum_1^{19} X_i\left[\frac{1}{2}\boldsymbol{E}_i(13)z^2 r^{e_i-2} + \boldsymbol{E}_i(7)zr^{e_i-1} + \boldsymbol{E}_i(1)r^{e_i}\right]\cos\theta$$
$$+ X_i\left[\boldsymbol{E}_i(10)zr^{e_i-1} + \boldsymbol{E}_i(4)r^{e_i}\right]\sin\theta, \tag{2.49}$$

with similar forms for u_θ and u_z where, for simplicity we have put

$$\begin{array}{lll} X_{16} = C, & \boldsymbol{E}_{16} = (\boldsymbol{Z}_{C1}^{\mathrm{T}}, \boldsymbol{0}, \boldsymbol{0}, \boldsymbol{0}, \boldsymbol{0})^{\mathrm{T}}, & \text{where } e_{16} = 2, \\ X_{17} = D, & \boldsymbol{E}_{17} = (\boldsymbol{0}, \boldsymbol{Z}_{D2}^{\mathrm{T}}, \boldsymbol{Z}_{D3}^{\mathrm{T}}, \boldsymbol{0}, \boldsymbol{0})^{\mathrm{T}}, & \text{where } e_{17} = 3, \\ X_{18} = E, & \boldsymbol{E}_{18} = (\boldsymbol{Z}_{E1}^{\mathrm{T}}, \boldsymbol{0}, \boldsymbol{0}, \boldsymbol{Z}_{E4}^{\mathrm{T}}, \boldsymbol{Z}_{E5}^{\mathrm{T}})^{\mathrm{T}}, & \text{where } e_{18} = 4, \\ X_{19} = W_0, & \boldsymbol{E}_{19} = (\boldsymbol{Z}_{W1}^{\mathrm{T}}, \boldsymbol{0}, \boldsymbol{0}, \boldsymbol{0}, \boldsymbol{0})^{\mathrm{T}}, & \text{where } e_{19} = 2. \end{array} \tag{2.50}$$

2.2. Boundary conditions

If we are to impose the condition that the surface $r = a$ of the cylinder is traction free, we need to compute the stress components σ_{rr}, $\sigma_{r\theta}$ and σ_{rz}. Each component contains terms in $\sin\theta$ and $\cos\theta$ with multipliers which are (at most) quadratic functions in z. Setting these terms equal to zero leads to 15 (linearly dependent) equations of the form

$$\sum_{i=1}^{15} X_i \boldsymbol{B}(e_i)\boldsymbol{E}_i = -C\boldsymbol{B}(2)\boldsymbol{Z}_C - D\boldsymbol{B}(3)\boldsymbol{Z}_D - E\boldsymbol{B}(4)\boldsymbol{Z}_E - W_0\boldsymbol{B}(2)\boldsymbol{Z}_W + \boldsymbol{R}_B, \tag{2.51}$$

where

$$\boldsymbol{R}_B = ac_{13}(C, 0, 0, 0, 0, 0, D, 0, 0, 0, 0, 0, E, 0, 0)^{\mathrm{T}}, \tag{2.52}$$

and the matrix $\boldsymbol{B}(q_i)$ has the partitioned form

$$\boldsymbol{B}(q) = \begin{pmatrix} a^{q-1}\boldsymbol{B}_{11}(q) & \boldsymbol{0} & \boldsymbol{0} & a^{q-1}\boldsymbol{B}_{14} & \boldsymbol{0} \\ \boldsymbol{0} & a^{q-1}\boldsymbol{B}_{22}(q) & a^{q-1}\boldsymbol{B}_{23} & \boldsymbol{0} & \boldsymbol{0} \\ \boldsymbol{0} & \boldsymbol{0} & a^{q-2}\boldsymbol{B}_{33}(q) & \boldsymbol{0} & \boldsymbol{0} \\ \boldsymbol{0} & \boldsymbol{0} & \boldsymbol{0} & a^{q-2}\boldsymbol{B}_{44}(q) & a^{q-2}\boldsymbol{B}_{45} \\ \boldsymbol{0} & \boldsymbol{0} & \boldsymbol{0} & \boldsymbol{0} & a^{q-3}\boldsymbol{B}_{55}(q) \end{pmatrix}, \tag{2.53}$$

and

$$\begin{aligned}
\boldsymbol{B}_{11}(q) &= \begin{pmatrix} c_{11}q + c_{12} & c_{12} & c_{14} \\ -c_{66} & c_{66}(q-1) & c_{56}q \\ -c_{56} & c_{56}(q-1) & c_{55}q \end{pmatrix}, \\
\boldsymbol{B}_{22}(q) &= \begin{pmatrix} c_{11}q + c_{12} & -c_{12} & -c_{14} \\ c_{66} & c_{66}(q-1) & c_{56}q \\ c_{56} & c_{56}(q-1) & c_{55}q \end{pmatrix}, \\
\boldsymbol{B}_{33}(q) &= \boldsymbol{B}_{11}(q-1), \quad \boldsymbol{B}_{44}(q) = \boldsymbol{B}_{22}(q-1), \\
\boldsymbol{B}_{55}(q) &= \boldsymbol{B}_{11}(q-2), \\
\boldsymbol{B}_{14} &= \begin{pmatrix} 0 & c_{14} & c_{13} \\ c_{56} & 0 & 0 \\ c_{55} & 0 & 0 \end{pmatrix}, \\
\boldsymbol{B}_{23} &= \boldsymbol{B}_{14}, \quad \boldsymbol{B}_{45} = \boldsymbol{B}_{14}.
\end{aligned} \tag{2.54}$$

In addition to imposing traction-free boundary conditions on the surface $r = a$ of the cylinder we also need to specify certain rigid-body displacements and rotations corresponding to the solutions 1, 4, 7 and 10. For the time being we shall suppose

$$X_1 = 0, \quad X_4 = 0, \quad X_7 = 0, \quad X_{10} = 0, \tag{2.55}$$

which gives a displacement of zero at the origin and a rotation of zero about the x and y axes at the origin.

Particular solutions of the system of equations (2.51) and (2.55) corresponding to simple bending, flexure and fourth-order bending are examined in the next sections.

2.3. Resultant forces and moments

The resultant forces and moments acting on the cross-section 'z' of the cylinder may be found for each eigenfunction solution with eigenvalue e_i and eigenvector $\boldsymbol{E}_i$. Using the definitions

$$\begin{aligned}
X &= \int_0^a \int_0^{2\pi} (\sigma_{rz}\cos\theta - \sigma_{\theta z}\sin\theta) r \, \mathrm{d}r \, \mathrm{d}\theta, \\
Y &= \int_0^a \int_0^{2\pi} (\sigma_{rz}\sin\theta + \sigma_{\theta z}\cos\theta) r \, \mathrm{d}r \, \mathrm{d}\theta, \\
Z &= \int_0^a \int_0^{2\pi} \sigma_{zz} r \, \mathrm{d}r \, \mathrm{d}\theta, \\
M_X &= \int_0^a \int_0^{2\pi} \sigma_{zz} r^2 \sin\theta \, \mathrm{d}r \, \mathrm{d}\theta, \\
M_Y &= -\int_0^a \int_0^{2\pi} \sigma_{zz} r^2 \cos\theta \, \mathrm{d}r \, \mathrm{d}\theta, \\
M_Z &= \int_0^a \int_0^{2\pi} \sigma_{\theta z} r^2 \, \mathrm{d}r \, \mathrm{d}\theta,
\end{aligned} \tag{2.56}$$

we find $Z = 0$ and $M_Z = 0$, so that these solutions correspond to a zero resultant longitudinal force and a zero torsional moment on each cross-section. As we remarked earlier, the axial extension and torsion solution separates from the bending solutions. The eigenfunction solution with eigenvalue e_i and eigenvector $\boldsymbol{E_i}$ generates the following resultant forces and moments:

$$\begin{aligned}
X &= \frac{\pi a^{e_i+1}}{e_i+1}(\mathbf{0},\boldsymbol{S}_1(e_i),\boldsymbol{S}_3,\mathbf{0},\mathbf{0})\boldsymbol{E}_i + z\frac{\pi a^{e_i}}{e_i}(\mathbf{0},\mathbf{0},\mathbf{0},\boldsymbol{S}_1(e_i-1),\boldsymbol{S}_3)\boldsymbol{E}_i,\\
Y &= \frac{\pi a^{e_i+1}}{e_i+1}(\boldsymbol{S}_2(e_i),\mathbf{0},\mathbf{0},\boldsymbol{S}_4,\mathbf{0})\boldsymbol{E}_i + z\frac{\pi a^{e_i}}{e_i}(\mathbf{0},\mathbf{0},S_2(e_i-1),\mathbf{0},\mathbf{0})\boldsymbol{E}_i + \frac{1}{2}z^2\frac{\pi a^{e_i-1}}{(e_i-1)}(\mathbf{0},\mathbf{0},\mathbf{0},\mathbf{0},\boldsymbol{S}_2(e_i-2))\boldsymbol{E_i},\\
M_X &= \frac{\pi a^{e_i+2}}{e_i+2}(\mathbf{0},\boldsymbol{S}_5(e_i),\boldsymbol{S}_7,\mathbf{0},\mathbf{0})\boldsymbol{E}_i + z\frac{\pi a^{e_i+1}}{e_i+1}(\mathbf{0},\mathbf{0},\mathbf{0},\boldsymbol{S}_5(e_i-1),\boldsymbol{S}_7)\boldsymbol{E}_i,\\
M_Y &= -\frac{\pi a^{e_i+2}}{e_i+2}(\boldsymbol{S}_6(e_i),\mathbf{0},\mathbf{0},\boldsymbol{S}_7,\mathbf{0})\boldsymbol{E}_i - z\frac{\pi a^{e_i+1}}{e_i+1}(\mathbf{0},\mathbf{0},S_6(e_i-1),\mathbf{0},\mathbf{0})\boldsymbol{E}_i - \frac{1}{2}z^2\frac{\pi a^{e_i}}{e_i}(\mathbf{0},\mathbf{0},\mathbf{0},\mathbf{0},\boldsymbol{S}_6(e_i-2))\boldsymbol{E}_i,
\end{aligned} \tag{2.57}$$

where

$$\begin{aligned}
\boldsymbol{S}_1(q) &= (c_{56}-(c_{14}q+c_{24}), c_{56}(q-1)+c_{24}, c_{55}q+c_{44}),\\
\boldsymbol{S}_2(q) &= (c_{14}q+c_{24}-c_{56}, c_{56}(q-1)+c_{24}, c_{55}q+c_{44}),\\
\boldsymbol{S}_3 &= (c_{55},-c_{44},-c_{34}),\\
\boldsymbol{S}_4 &= (c_{55},c_{44},c_{34}),\\
\boldsymbol{S}_5(q) &= (c_{13}q+c_{23},-c_{23},-c_{34}),\\
\boldsymbol{S}_6(q) &= (c_{13}q+c_{23},c_{23},c_{34}),\\
\boldsymbol{S}_7 &= (0,c_{34},c_{33}).
\end{aligned} \tag{2.58}$$

Solutions corresponding to the zero eigenvalue, namely 1, 4, 7 and 10, are rigid-body displacements with zero resultant forces and moments.

The additional resultant force and moment terms due to the simple bending (C), flexure (D) and fourth-order bending terms (E) in the original displacement field (2.5) are

$$\begin{aligned}
&X = 0, \quad Y = -\pi c_{34}\frac{a^3}{3}\left(C + Dz + \frac{1}{2}Ez^2\right), \quad Z = 0,\\
&M_X = 0, \quad M_Y = \pi c_{33}\frac{a^4}{4}\left(C + Dz + \frac{1}{2}Ez^2\right), \quad M_Z = 0.
\end{aligned} \tag{2.59}$$

The particular solutions (2.14), (2.16), (2.18) and (2.23) also contribute to the resultant forces and moments through the formulae (2.57) by using the extended eigenvector representation (2.50).

The following sections examine the simple bending, flexure and the effect of a uniform transverse load on a cable.

3. Simple bending of a cylinder

In this section we examine the case of a helically reinforced cylinder or cable ($0 \leqslant z \leqslant z_0$) which is bent into a parabolic shape by forces and moments applied to its ends whilst the surface $r = a$ of the cylinder remains traction free. We suppose the axis of the cylinder is bent into a parabolic shape with curvature C and the constants D, E and W_0 in (2.6) are taken to be zero. Assuming the zero rigid-body displacement conditions (2.55) hold at the origin $(0,0,0)$, the zero traction conditions on the surface of the cylinder reduce to Eqs. (2.51), in which $D = 0$, $E = 0$ and $W_0 = 0$. In this case, since only the first three components of $\boldsymbol{Z}_C$ are non-zero, the term $\boldsymbol{B}(2)\boldsymbol{Z}_C$ on the right-hand side of (2.51) only has non-zero values in its first three components. If we examine the left-hand side of (2.51) this indicates we should be able to solve the system by selecting those eigenvectors with components 4 to 15 equal to zero.

Only the first three eigenvectors have this form, hence we can reduce the system to

$$X_2 a^{q_2-1}\boldsymbol{B}_{11}(q_2)\big(1, V_2^{\mathrm{T}}(q_2)\big)^{\mathrm{T}} + X_3 a^{q_3-1}\boldsymbol{B}_{11}(q_3)\big(1, V_2^{\mathrm{T}}(q_3)\big)^{\mathrm{T}} = -Ca\boldsymbol{B}_{11}(2)\boldsymbol{Z}_c + c_{13}a(C,0,0)^{\mathrm{T}}, \tag{3.1}$$

remembering we have set $X_1 = 0$ and that q_2 and q_3 are the two positive eigenvalues of $\boldsymbol{M}_{11}(q)$.

This may be shown to be a linearly dependent set of three equations in two variables. If we observe that

$$\boldsymbol{M}_{11}(q) = q\boldsymbol{B}_{11}(q) - \boldsymbol{L}_{11}(q), \tag{3.2}$$

by using (2.54) and the Appendix B, then

$$\boldsymbol{L}_{11}(q) = \begin{pmatrix} c_{12}q + c_{22} + c_{66} & -c_{66}q + c_{22} + c_{66} & -c_{56}q + c_{24} \\ c_{12}q + c_{22} + c_{66} & -c_{66}q + c_{22} + c_{66} & -c_{56}q + c_{24} \\ c_{14}q + c_{24} & c_{24} & c_{44} \end{pmatrix} \tag{3.3}$$

and the first two rows of this matrix are identical. If we substitute for $\boldsymbol{B}_{11}(q)$ in (3.1) and use the fact that the vectors $(1, V_2^{\mathrm{T}}(q_i))^{\mathrm{T}}$ are eigenvectors of $\boldsymbol{M}_{11}(q_i)$, we see that the left-hand side of (3.1) reduces to

$$X_2 a^{q_2-1}\frac{1}{q_2}\boldsymbol{L}_{11}(q_2)(1, V_2^{\mathrm{T}}(q_2))^{\mathrm{T}} + X_3 a^{q_3-1}\frac{1}{q_3}\boldsymbol{L}_{11}(q_3)(1, V_2^{\mathrm{T}}(q_3))^{\mathrm{T}}$$

and the first two rows of this expression are identical.

Similarly, if we put $2\boldsymbol{B}_{11}(2) = \boldsymbol{M}_{11}(2) + \boldsymbol{L}_{11}(2)$ and observe that $\boldsymbol{Z}_C = \boldsymbol{M}_{11}^{-1}(2)\boldsymbol{R}_{10}$ from (2.15), the right-hand side of (3.1) reduces to

$$\tfrac{1}{2}Ca(c_{23}, c_{23}, c_{34})^{\mathrm{T}} - \tfrac{1}{2}Ca\boldsymbol{L}_{11}(2)\boldsymbol{M}_{11}^{-1}(2)\boldsymbol{R}_{10} \tag{3.4}$$

and the first two components are identical.

Hence the multipliers X_2 and X_3 satisfy the second and third equations of

$$\begin{aligned} &X_2\frac{a^{q_2-1}}{q_2}\boldsymbol{L}_{11}(q_2)(1, V_2^{\mathrm{T}}(q_2))^{\mathrm{T}} + X_3\frac{a^{q_3-1}}{q_3}\boldsymbol{L}_{11}(q_3)(1, V_2^{\mathrm{T}}(q_3))^{\mathrm{T}} \\ &\quad = \frac{1}{2}Ca(c_{23}, c_{23}, c_{34})^{\mathrm{T}} - \frac{1}{2}Ca\boldsymbol{L}_{11}(2)\boldsymbol{M}_{11}^{-1}(2)\boldsymbol{R}_{10}, \end{aligned} \tag{3.5}$$

where

$$\boldsymbol{R}_{10} = (2c_{13} - c_{23}, -c_{23}, -c_{34})^{\mathrm{T}} \tag{3.6}$$

and $(1, V_2^{\mathrm{T}}(q_i))^{\mathrm{T}}$ are the eigenvectors of $\boldsymbol{M}_{11}(q_i)$ $(i = 2, 3)$ and satisfy (2.34).

For simple bending, the resultant forces are given by (2.57) as

$$X = 0, \quad Y = X_2\frac{\pi a^{q_2+1}}{q_2+1}\boldsymbol{S}_2(q_2)\boldsymbol{Z}_1^{(2)} + X_3\frac{\pi a^{q_3+1}}{q_3+1}\boldsymbol{S}_2(q_3)\boldsymbol{Z}_1^{(3)} + C\frac{\pi a^3}{3}\boldsymbol{S}_2(2)\boldsymbol{Z}_{C_1} - C\pi c_{34}\frac{a^3}{3}. \tag{3.7}$$

But $\boldsymbol{S}_2(q)$ is equal to the third row of $(q+1)\boldsymbol{B}_{11}(q) - \boldsymbol{M}_{11}(q)$ and, when this is substituted into (3.6) and we use (3.1), the value of Y reduces to $-(1/3)C\pi a^3[\boldsymbol{M}_{11}^{(3)}(2)\boldsymbol{Z}_C + c_{34}]$ which is easily shown to be zero. Here $\boldsymbol{M}_{11}^{(3)}$ is the third row of $\boldsymbol{M}_{11}$. Hence the simple bending deformation is maintained by the application of zero resultant forces $X \equiv 0$, $Y \equiv 0$ to the end-face of the cylinder and the constant moment (from (2.57)) given by the following:

$$M_X = 0, \quad M_Y = -X_2\frac{\pi a^{q_2+2}}{q_2+2}\boldsymbol{S}_6(q_2)\boldsymbol{Z}_1^{(2)} - X_3\frac{\pi a^{q_3+2}}{q_3+2}\boldsymbol{S}_6(q_3)\boldsymbol{Z}_1^{(3)} - C\frac{\pi a^4}{4}\boldsymbol{S}_6(2)\boldsymbol{Z}_{C_1} + C\pi\frac{a^4}{4}c_{33}. \tag{3.8}$$

Hence application of a bending moment to the end-face of this anisotropic cylinder causes it to bend into a parabolic curve in the plane orthogonal to the bending moment.

In the special case of a helically reinforced cable, Jolicoeur and Cardou (1994) have given two sets of strain compliances. When the strain compliances of their material 1 (which corresponds to a 15° winding angle) are inverted to produce stiffnesses they yield the symmetric matrix

$$10^{-9}\boldsymbol{C} = \begin{pmatrix} 9.922 & 1.148 & 4.354 & -0.925 & 0 & 0 \\ \dots & 9.199 & 7.315 & -0.899 & 0 & 0 \\ \dots & \dots & 48.32 & -10.394 & 0 & 0 \\ \dots & \dots & \dots & 5.240 & 0 & 0 \\ 0 & 0 & 0 & 0 & 2.134 & 0.4999 \\ 0 & 0 & 0 & 0 & \dots & 3.866 \end{pmatrix}, \tag{3.9}$$

measured in $\mathrm{N/m^2}$.

The corresponding eigenvalues are

$$q_1 = 0, \quad q_2 = 1.50547, \quad q_3 = 2.10654. \tag{3.10}$$

The eigenvectors $\boldsymbol{Z}_1^{(2)}$ and $\boldsymbol{Z}_1^{(3)}$ and the particular solution $\boldsymbol{Z}_C$ are

$$\boldsymbol{Z}_1^{(2)} = (1, 2.217, 10.826)^{\mathrm{T}}, \quad \boldsymbol{Z}_1^{(3)} = (1, 12.369, -6.464)^{\mathrm{T}}, \quad \boldsymbol{Z}_C = (0.8198, 6.712, -1.1499)^{\mathrm{T}}.$$

The scaling factors $a^{q_2-1}X_2$ and $a^{q_3-1}X_3$ which satisfy (3.1) are

$$a^{q_2-1}X_2 = -0.2449a, \quad a^{q_3-1}X_3 = -0.462a \tag{3.11}$$

and hence the deformation field in the cylinder is

$$\begin{aligned} u_r &= C[0.8198r^2 + \tfrac{1}{2}z^2 - 0.2449a^2(r/a)^{q_2} - 0.4621a^2(r/a)^{q_3}]\cos\theta, \\ u_\theta &= C[6.712r^2 - \tfrac{1}{2}z^2 - 0.5431a^2(r/a)^{q_2} - 5.716a^2(r/a)^{q_3}]\sin\theta, \\ u_z &= C[-1.149r^2 - 2.652a^2(r/a)^{q_2} + 2.987a^2(r/a)^{q_3}]\sin\theta - Czr\cos\theta. \end{aligned} \tag{3.12}$$

The axis of the cylinder has been bent into a parabolic curve with curvature C in the (x, z)-plane. This is maintained by the constant bending moment

$$M_Y = 23.154 \times 10^9 a^4 C \ \mathrm{N\,m}, \tag{3.13}$$

where it should be noted that C has the dimension of L^{-1} and lengths should be measured in metres for consistency with the elastic constants. This result yields a bending stiffness of 889 $\mathrm{N\,m^2}$ for a solid cable of 14 mm radius which compares well with Jolicoeur and Cardou's result of 707 $\mathrm{N\,m^2}$ for a hollow composite cable $2 \leqslant r \leqslant 14$ mm with the same external radius.

The solution for bending in the (y, z)-plane under the bending moment M_X can be obtained by replacing θ by $\theta + \pi/2$ in the above solutions. Note that this yields a negative value for M_X.

4. Flexure of a cylinder

In this section we consider the case of a helically reinforced cylinder which is bent into a cubic shape of the form $u_x = (1/6)Dz^3$ in the (x, z)-plane by the action of forces and moments applied to its ends. We assume the surface of the cylinder is traction-free and that the zero rigid-body displacement conditions (2.55) hold at the origin. In this case we are looking for a solution of the boundary conditions (2.51) in which $C = 0$, $E = 0$ and $W_0 = 0$. We shall find that this is only possible if, in addition to a resultant shear force Y and moment M_Y, a constant moment M_X is applied to the end-face of the cylinder, indicating that the cylinder also wants to go into a state of simple bending in the (y,z)-plane. Thus the effect of the helical winding manifests itself in this out-of-plane bending under flexure. The combined solution of flexure in the (x,z)-plane and simple bending in the (y,z)-plane, the equivalent of the cantilever problem, is then found.

When $C=0$, $E=0$, and $W_0=0$ then the right-hand side of (2.51) reduces to

$$-D\boldsymbol{B}(3)\boldsymbol{Z}_D + c_{13}a(\boldsymbol{0},\boldsymbol{0},D,0,0,0,\boldsymbol{0},\boldsymbol{0})^{\mathrm{T}},$$

where $\boldsymbol{Z}_D$ is defined by (2.18).

Hence the right-hand side of (2.52) only has non-zero components in rows 4 to 9. Given the form of the eigenvectors, we might expect the solution to depend only on the eigenvector solutions 4 to 9 and hence the boundary conditions will reduce to

$$\sum_{i=4}^{9} X_i\boldsymbol{B}(e_i)\boldsymbol{E}_i = -D\boldsymbol{B}(3)\boldsymbol{Z}_D + c_{13}a(\boldsymbol{0},\boldsymbol{0},D,0,0,0,\boldsymbol{0},\boldsymbol{0})^{\mathrm{T}}. \tag{4.1}$$

In addition, if we fix the rigid-body displacement X_4 and the rotation X_7 to be zero at the origin, the system reduces to the following six equations in four unknowns:

$$\begin{aligned} X_5a^{q_2-1}\boldsymbol{B}_{22}(q_2)\boldsymbol{Z}_2^{(5)} + X_6a^{q_3-1}\boldsymbol{B}_{22}(q_3)\boldsymbol{Z}_2^{(6)} + X_8\left[\boldsymbol{B}_{22}(1+q_2)\boldsymbol{Z}_2^{(8)} + \boldsymbol{B}_{23}(1+q_2)\boldsymbol{Z}_3^{(8)}\right]a^{q_2-1} \\ + X_9\left[\boldsymbol{B}_{22}(1+q_3)\boldsymbol{Z}_2^{(9)} + \boldsymbol{B}_{23}(1+q_3)\boldsymbol{Z}_3^{(9)}\right]a^{q_3-1} = -Da^2(\boldsymbol{B}_{22}(3)\boldsymbol{Z}_{D2} + \boldsymbol{B}_{23}(3)\boldsymbol{Z}_{D3}) \end{aligned} \tag{4.2}$$

$$X_8a^{q_2-2}\boldsymbol{B}_{33}(1+q_2)\boldsymbol{Z}_3^{(8)} + X_9a^{q_3-2}\boldsymbol{B}_{33}(1+q_3)\boldsymbol{Z}_3^{(9)} = -a\boldsymbol{B}_{33}(3)\boldsymbol{Z}_{D3} + c_{13}aD(1,0,0)^{\mathrm{T}}. \tag{4.3}$$

But we have shown that $\boldsymbol{B}_{33}(1+q_i) = \boldsymbol{B}_{11}(q_i)$ and $\boldsymbol{Z}_3^{(8)} = \boldsymbol{Z}_1^{(2)}$, $\boldsymbol{Z}_3^{(9)} = \boldsymbol{Z}_1^{(3)}$, $\boldsymbol{Z}_{D3} = \boldsymbol{Z}_{C1}$, so that the system of equations (4.3) is identical to (3.1) on replacing X_8 by aX_2 and X_9 by aX_3 and C by D. We have shown that the three equations in (3.1) are linearly dependent and hence we find

$$X_8 = DaX_2/C, \quad X_9 = DaX_3/C, \tag{4.4}$$

where X_2 and X_3 are defined by (3.4).

The variables X_5 and X_6 must then satisfy the three equations in (4.2). The first two terms on the left-hand side of (4.2) are

$$X_5a^{q_2-1}\boldsymbol{B}_{22}(q_2)\boldsymbol{Z}_2^{(5)} + X_6a^{q_3-1}\boldsymbol{B}_{22}(q_3)\boldsymbol{Z}_2^{(6)}, \tag{4.5}$$

but, as in (3.2),

$$\boldsymbol{M}_{22}(q) = q\boldsymbol{B}_{22}(q) - \boldsymbol{L}_{22}(q), \tag{4.6}$$

where

$$\boldsymbol{L}_{22}(q) = \begin{pmatrix} c_{12}q + c_{22} + c_{66} & c_{66}q - c_{22} - c_{66} & c_{56}q - c_{24} \\ -c_{12}q - c_{22} - c_{66} & -c_{66}q + c_{22} + c_{66} & -c_{56}q + c_{24} \\ -c_{14}q - c_{24} & c_{24} & c_{44} \end{pmatrix} \tag{4.7}$$

and $\boldsymbol{Z}_2^{(5)}$ and $\boldsymbol{Z}_2^{(6)}$ are eigenvectors of $\boldsymbol{M}_{22}(q_2)$, $\boldsymbol{M}_{22}(q_3)$. Hence the X_5 and X_6 terms on the left-hand side of (4.2) reduce to

$$X_5\frac{a^{q_2-1}}{q_2}\boldsymbol{L}_{22}(q_2)\boldsymbol{Z}_2^{(5)} + X_6\frac{a^{q_3-1}}{q_3}\boldsymbol{L}_{22}(q_3)\boldsymbol{Z}_2^{(6)}, \tag{4.8}$$

in which rows one and two are identical in form but opposite in sign. If these two equations are added together, then X_5 and X_6 cancel from the equation and the remaining terms turn out to be identical to the third equation of (4.3). Hence we need only solve the second and third equations of (4.2) for X_5 and X_6.

If we consider the case of a helically reinforced cable and use Jolicoeur and Cardou's stiffnesses (see (3.9)), the eigenvectors which occur in the flexure problem have the non-zero components

$$\begin{aligned} \boldsymbol{Z}_1^{(5)} &= (1, -2.2173, -10.827)^{\mathrm{T}}, & \boldsymbol{Z}_1^{(6)} &= (1, -12.369, 6.464)^{\mathrm{T}}, \\ \boldsymbol{Z}_2^{(8)} &= (-1.293, -22.574, 29.227)^{\mathrm{T}}, & \boldsymbol{Z}_3^{(8)} &= (1, 2.2173, 10.827)^{\mathrm{T}}, \\ \boldsymbol{Z}_2^{(9)} &= (1.462, 9.388, -22.712)^{\mathrm{T}}, & \boldsymbol{Z}_3^{(9)} &= (1, 12.369, -6.464)^{\mathrm{T}}, \end{aligned} \tag{4.9}$$

and the particular solution has

$$\boldsymbol{Z}_{D2} = (0.372, 2.249, -6.173)^{\mathrm{T}}, \quad \boldsymbol{Z}_{D3} = (0.820, 6.712, -1.150)^{\mathrm{T}}. \tag{4.10}$$

The flexure solution gives rise to the following multipliers of the eigenvectors

$$\begin{aligned} &X_5 = 0.0139a^{3-q_2}, \quad X_6 = 0.291a^{3-q_3}, \\ &X_8 = -0.245a^{2-q_2}, \quad X_9 = -0.462a^{2-q_3}, \end{aligned} \tag{4.11}$$

and generates a displacement field of the form

$$\begin{aligned} u_r = {} & D\left[\frac{1}{6}z^3 + 0.8198zr^2 - 0.245a^2z\left(\frac{r}{a}\right)^{q_2} - 0.462a^2z\left(\frac{r}{a}\right)^{q_3}\right]\cos\theta \\ & + D\left[0.3718r^3 + 0.0139a^3\left(\frac{r}{a}\right)^{q_2} + 0.291a^3\left(\frac{r}{a}\right)^{q_3} + 0.316a^3\left(\frac{r}{a}\right)^{1+q_2} - 0.6760a^3\left(\frac{r}{a}\right)^{1+q_3}\right]\sin\theta, \end{aligned} \tag{4.12}$$

with similar expressions for u_θ and u_z.

These deformations correspond to the centre-line of the cable having the shape $u_x = (1/6)Dz^3$ in the (x, z)-plane and are maintained by the following resultant forces and moments acting on the cross-section of the cylinder

$$\begin{aligned} &X = -23.154 \times 10^9 Da^4, \quad Y = 0, \\ &M_X = -45.035 \times 10^9 Da^5, \quad M_Y = 23.154 \times 10^9 Dza^4, \end{aligned} \tag{4.13}$$

measured in Newtons and N m. The constant moment M_X has to be applied to prevent the rod bending in the (y, z)-plane.

This solution may be combined with the simple bending solution (found in Section 3) to find the deformation of a cylinder which is built-in (in a Saint-Venant sense) at $z = 0$ and has a uniform resultant shear force X_0 and zero bending moments applied at the end $z = z_0$ of the cylinder. We achieve this by choosing D to match the applied shear force X_0 using $(4.13)_1$, allowing the cable to undergo simple bending in the (x, z)-plane under the bending moment $M_Y = X_0 z_0$ (applied to the end-face $z = z_0$) which is equal and opposite to that in $(4.13)_4$ together with a simple bending in the (y, z)-plane under an equal and opposite bending moment to M_x in $(4.13)_3$, in this case $M_X = -1.945X_0 a$.

The resultant forces and moments in the cylinder at the cross-section 'z' reduce to

$$\begin{aligned} &X = X_0, \quad Y = 0, \quad Z = 0, \\ &M_X = 0, \quad M_Y = X_0(z_0 - z), \quad M_Z = 0, \end{aligned} \tag{4.14}$$

and the corresponding deformation of the axis $(r = 0)$ of the cylinder in Cartesian co-ordinates is

$$\begin{aligned} &u_x = 0.007198 \times 10^{-9} X_0 z^2 (3z_0 - z)/a^4, \\ &u_y = 0.0420 \times 10^{-9} X_0 z^2/a^3, \quad u_z = 0, \end{aligned} \tag{4.15}$$

measured in metres, see Fig. 1. This graph gives the non-dimensional deflections $10^{-6}c_{33}au_x/X_0$, displayed as a continuous line, and $10^{-6}c_{33}au_y/X_0$ for a cylinder of length $100a$. Hence, under flexure, the cylinder bends

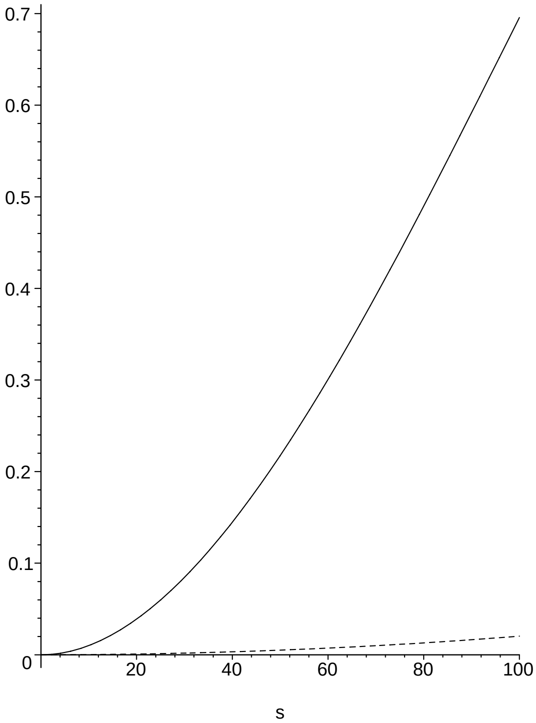

Fig. 1. Flexure of a cylindrical cantilever of length $z_0 = 100a$ by a resultant force $X_0\boldsymbol{i}$ applied to its end. The non-dimensional deflections $(10^{-6}ac_{33}/X_0)u_x$ and $(10^{-6}ac_{33}/X_0)u_y$ are plotted as functions of $s = z/a$.

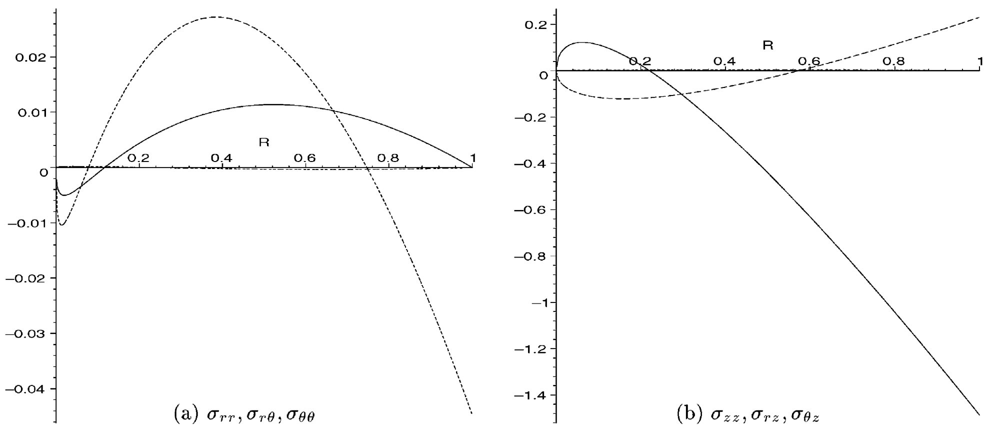

Fig. 2. Flexure of a cylindrical cantilever of length $100a$ by a resultant force $X_0\boldsymbol{i}$ applied to its end. The $\cos\theta$ components of the non-dimensional stress field on $z = 0$.

up in the (x, z)-plane and to the right in the (y, z)-plane. This cable has been manufactured with an anti-clockwise helical winding of 15° relative to the axis of the cylinder. If the winding is made clockwise with an angle of 15°, the bend in the (y, z)-plane is reversed.

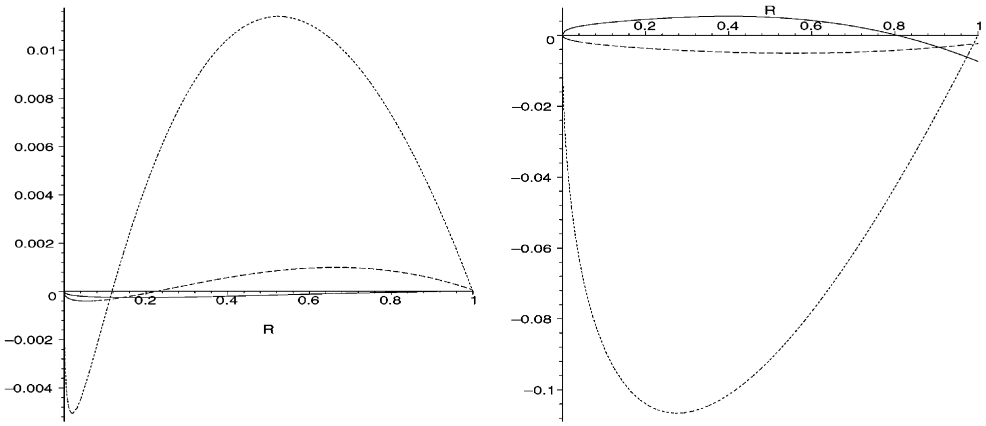

(a) $\sigma_{rr}, \sigma_{r\theta}, \sigma_{\theta\theta}$ (b) $\sigma_{zz}, \sigma_{rz}, \sigma_{\theta z}$

Fig. 3. Flexure of a cylindrical cantilever of length $100a$ by a resultant force $X_0\boldsymbol{i}$ applied to its end. The $\sin\theta$ components of the stress field on $z = 0$.

The stress field on the cross-section $z = 0$ for a cantilever of length $100a$ is shown on Figs. 2 and 3. Each stress component has the form of $f(r)\cos\theta + g(r)\sin\theta$ for $0 \leqslant r \leqslant a$. Fig. 2 plots the $\cos\theta$ components of the stress field, scaled by $a^3/(X_0 z_0)$, as a function of r/a. Fig. 3 plots the $\sin\theta$ components of the stress field scaled by $a^3/(X_0 z_0)$, as a function of r/a.

The continuous lines denote σ_{rr} and σ_{zz}. The dotted lines denoting $\sigma_{r\theta}$ and σ_{rz} go to zero at $r = a$. The dashed lines denote $\sigma_{\theta\theta}$ and $\sigma_{\theta z}$. This notation has been used on all figures involving the stress components. We note that σ_{zz} is the largest stress component and that σ_{rr}, $\sigma_{\theta\theta}$, σ_{zz}, $\sigma_{\theta z}$ depend largely on $\cos\theta$, whilst σ_{rz} and $\sigma_{r\theta}$ depend largely on $\sin\theta$. The cable is principally bending by flexure in the (x, z)-plane which corresponds to $\theta = 0$.

The flexure solution for the (y, z)-plane is easily found on replacing θ by $\theta + \pi/2$.

5. Body force solutions

A particular solution was obtained in Section 2 corresponding to the case when a constant body force of magnitude W_0 per unit volume acts in the x-direction. This produces a fourth-order deflection of the centreline of the rod. The boundary conditions (2.51) become

$$\sum_{i=1}^{15} X_i \boldsymbol{B}(e_i)\boldsymbol{E}_i + E\boldsymbol{B}(4)\boldsymbol{Z}_E - \boldsymbol{R}_B = -W_0 \boldsymbol{B}(2)\boldsymbol{Z}_W, \tag{5.1}$$

in which we have taken C and D equal to zero. If we fix the displacement field and the rotations to be zero at the origin, the problem reduces to satisfying the 15 equations in (5.1). We have 11 of the constants X_i and the constant E at our disposal.

As in the previous sections, this is a linearly dependent set of equations and a unique solution may be found which corresponds to fourth-order bending in the (x, z)-plane. This deformation can only be maintained by the application of the resultant forces X_{bf} and Y_{bf}, and resultant moments $M_{X\,\mathrm{bf}}$ and $M_{Y\,\mathrm{bf}}$ at the end $z = z_0$ of the rod. In the case of the cable modelled using Jolicoeur and Cardou's constants (3.9), the multipliers X_i and E are

$$X_1 = 0, \quad X_2 = -0.094a^{2-q_2}, \quad X_3 = 0.057a^{2-q_3}, \quad X_4 = X_5 = X_6 = 0, \quad X_7 = X_8 = X_9 = 0,$$
$$X_{10} = 0, \quad X_{11} = 0.0019a^{1-q_2}, \quad X_{12} = 0.0395a^{1-q_3}, \quad X_{13} = 0, \quad X_{14} = -0.0332a^{-q_2},$$
$$X_{15} = -0.0627a^{-q_3}, \quad E = 0.1357/a^2, \tag{5.2}$$

where each term should be multiplied by $10^{-9}W_0$ to put it into dimensional form and W_0 is measured in N/m^3. The resultants necessary to maintain this deformation in the (x, z)-plane have the following values on $z = z_0$:

$$\begin{aligned} X_{\text{bf}} &= -\pi a^2 z_0 W_0, \quad Y_{\text{bf}} = -6.110a^3 W_0, \\ M_{X\,\text{bf}} &= -6.110a^3 z_0 W_0, \quad M_{Y\,\text{bf}} = \left(\frac{1}{2}\pi a^2 z_0^2 - 2.738a^4\right) W_0. \end{aligned} \tag{5.3}$$

5.1. The cantilever problem

The resultant forces and moments in (5.3) may be removed by combining this solution with bending and flexural deformations in the (x, z) and (y, z) planes.

The combined solutions are of the form

$$\boldsymbol{u} = \boldsymbol{u}_{\text{bf}} + C1\boldsymbol{u}_{\text{sb}} + C2\boldsymbol{u}_{\text{sb2}} + D1\boldsymbol{u}_{\text{fl}} + D2\boldsymbol{u}_{\text{fl2}}, \tag{5.4}$$

where $\boldsymbol{u}_{\text{bf}}$ is the body force field of the type (2.6) found by solving (5.1), $\boldsymbol{u}_{\text{sb}}$ is the simple bending field and $\boldsymbol{u}_{\text{fl}}$ the flexure field found in the previous sections. The fields $\boldsymbol{u}_{\text{sb2}}$ and $\boldsymbol{u}_{\text{fl2}}$ are the corresponding bending and flexure fields in the (y, z)-plane. In the cantilever problem we must choose the multiplying constants to ensure the end $z = z_0$ of the cylinder is unloaded and the end $z = 0$ is built-in in a Saint-Venant sense. The corresponding constants are

$$\begin{aligned} D1 &= -X_{\text{bf}}/X_{\text{fl}}, \quad D2 = Y_{\text{bf}}/X_{\text{fl}}, \\ C1 &= -(M_{Y\,\text{bf}} + D1 M_{Y\,\text{fl}} - D2 M_{X\,\text{fl}})/b_{\text{s}}, \\ C2 &= -(M_{X\,\text{bf}} + D1 M_{X\,\text{fl}} + D2 M_{Y\,\text{fl}})/b_{\text{s}}, \end{aligned} \tag{5.5}$$

where X_{fl}, $M_{X\,\text{fl}}$, $M_{Y\,\text{fl}}$ are the forces and moments which occur in Eq. (4.13) of the flexure problem and b_{s} is the bending stiffness given in (3.13) of the bending problem.

The resultant forces and moments in the rod become

$$X = W_0 \pi a^2 (z_0 - z), \quad Y = 0, \quad Z = 0, \quad M_X = 0, \quad M_Y = \tfrac{1}{2} W_0 \pi a^2 (z - z_0)^2, \quad M_Z = 0. \tag{5.6}$$

Using Jolicoeur and Cardou's constants (3.9), the displacement field on the axis of the cylinder is

$$\begin{aligned} u_x &= 5.653 \times 10^{-12} W_0 a^2 \left(\frac{z}{a}\right)^2 \left(\left(\frac{z}{a}\right)^2 - 4\left(\frac{zz_0}{a^2}\right) + 6\left(\frac{z_0}{a}\right)^2 - 34.938\right), \\ u_y &= 43.983 \times 10^{-12} W_0 a^2 \left(\frac{z}{a}\right)^2 \left(\frac{3z_0 - z}{a}\right). \end{aligned} \tag{5.7}$$

The non-dimensional deflections of a cylindrical cantilever of length $z_0 = 100a$ under the body force $W_0\boldsymbol{i}$ per unit volume are shown on Fig. 4. The deflections are scaled by $10^{-6}ac_{33}/(\pi a^2 z_0 W_0)$ and are plotted as functions of $s = z/a$.

The $\cos\theta$ components of the non-dimensional stress field on the cross-section $z = 0$ are given on Fig. 5 and the corresponding $\sin\theta$ components on Fig. 6. Again the stress components have been scaled by $a^2/(\pi a^2 z_0 W_0)$ where the denominator is the total 'weight' of the cylinder. Note that the largest stress is the $\cos\theta$ component of σ_{zz} on Fig. 5 and the principal bending direction is in the $\theta = 0$ plane.

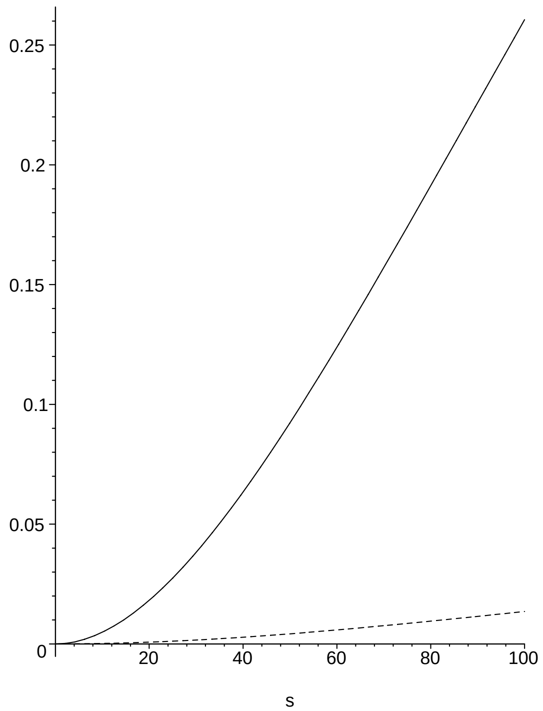

Fig. 4. Deflection of a cylindrical cantilever of length $z_0 = 100a$ by a body force W_0. The non-dimensional deflections $(10^{-6}ac_{33}/(\pi a^2 z_0 W_0))(u_x, u_y)$ are plotted as functions of $s = z/a$.

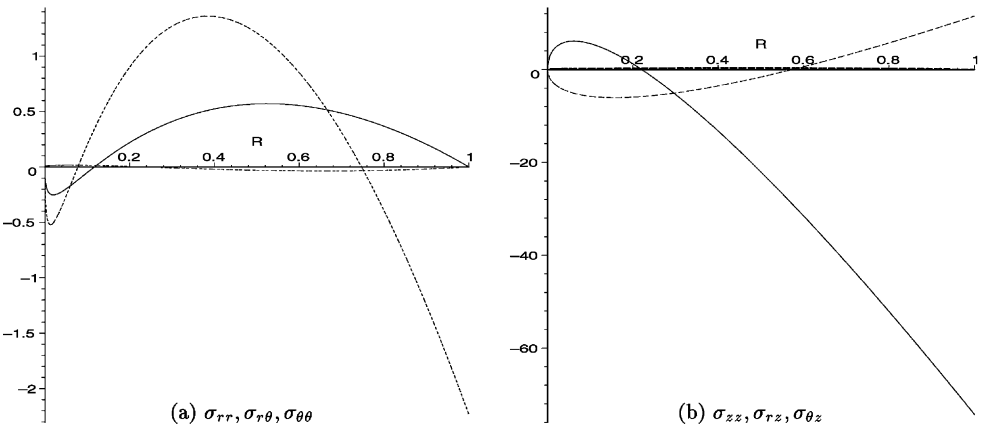

Fig. 5. Deflection of a cylindrical cantilever of length $z_0 = 100a$ by a body force W_0. The $\cos\theta$ components of the non-dimensional stress field on $z = 0$ are plotted as a function of $R = r/a$.

5.2. The catenary problem

In a similar manner we can examine the transverse deflections of a cable supported at both ends. The full catenary problem, of course, involves a combination of a finite deflection of the cable, and the extensional behaviour modelled by Blouin and Cardou (1989). The Saint-Venant type solutions for the linear elastic

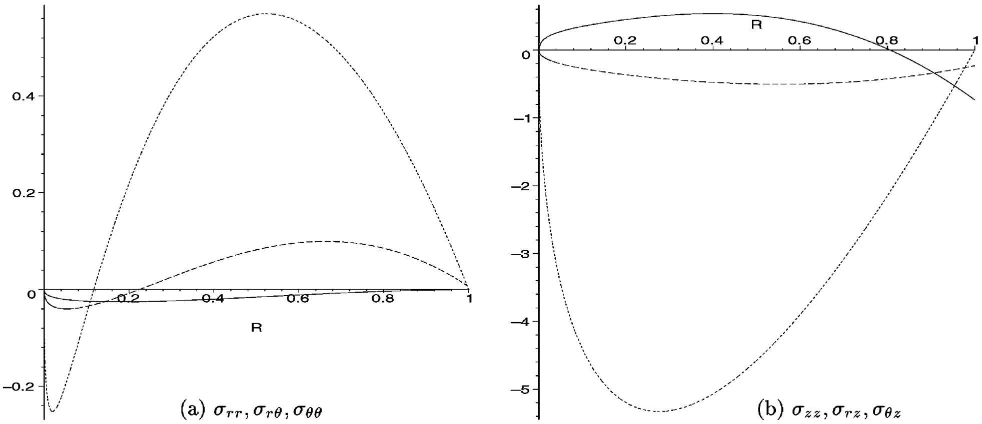

Fig. 6. Deflection of a cylindrical cantilever of length $z_0 = 100a$ by a body force W_0. The $\sin\theta$ components of the non-dimensional stress field on $z = 0$ are plotted as a function of $R = r/a$.

small transverse deflections under self-weight of the cable are all that will be modelled here. To find the solution for a cable which is simply supported at both ends we must permit rotations to take place at each end so that the displacement field $\boldsymbol{u}$ has the representation

$$\boldsymbol{u} = \boldsymbol{u}_{\mathrm{bf}} + C_1\boldsymbol{u}_{\mathrm{sb}} + C_2\boldsymbol{u}_{\mathrm{sb2}} + D_1\boldsymbol{u}_{\mathrm{fl}} + D_2\boldsymbol{u}_{\mathrm{fl2}} + R_1\boldsymbol{u}_7 + R_2\boldsymbol{u}_{10}, \tag{5.8}$$

where $\boldsymbol{u}_7$ and $\boldsymbol{u}_{10}$ are the displacement fields given in Section 2.1 corresponding to the eigenvector solutions 7 and 10, which correspond to rotations at the origin and $\boldsymbol{u}_{\mathrm{bf}}$, $\boldsymbol{u}_{\mathrm{sb}}$ etc. are the displacement fields defined in Eq. (5.4). We select these coefficients so that one of the following two sets of boundary conditions is satisfied at $z = 0$ and $z = z_0$

$$\begin{aligned} &(\mathrm{a}) \quad u_x = 0, \quad u_y = 0, \quad u_{y,z} = 0, \quad M_Y = 0, \\ &(\mathrm{b}) \quad u_x = 0, \quad u_y = 0, \quad M_X = 0, \quad M_Y = 0. \end{aligned} \tag{5.9}$$

In case (a) the cable is permitted to rotate at its ends in the (x, z)-plane only, as if it were held in a small pulley, and in case (b) the ends are simply supported and free to rotate about the x and y axes.

Case (a): The solution subject to the boundary conditions

$$u_x = 0, \quad u_y = 0, \quad u_{y,z} = 0, \quad M_Y = 0, \tag{5.10}$$

at the ends $z = 0, z = z_0$ yields a displacement which lies entirely in the (x, z)-plane ($u_y \equiv 0$) and is supported by the forces and moments

$$X = \frac{\pi}{2}W_0a^2(z_0 - 2z), \quad Y = -6.110W_0a^3, \quad M_X = 3.055W_0a^3(z_0 - 2z), \quad M_Y = -\frac{\pi}{2}W_0a^2z(z_0 - z). \tag{5.11}$$

Hence the deformation is possible if equal and opposite reaction forces $\mp 6.110W_0a^3$ acting in the y-direction and reaction moments $M_X = \pm 3.055W_0a^3z_0$ are applied at the supports at $z = 0$ and $z = z_0$, in addition to the reactions $(-\pi/2)W_0a^2z_0$ acting in the x-direction which support the load.

The scaled displacement field is shown on Fig. 7.

Case (b): The cable is subject to the (simply-supported) boundary conditions

$$u_x = 0, \quad u_y = 0, \quad M_X = 0, \quad M_Y = 0,$$

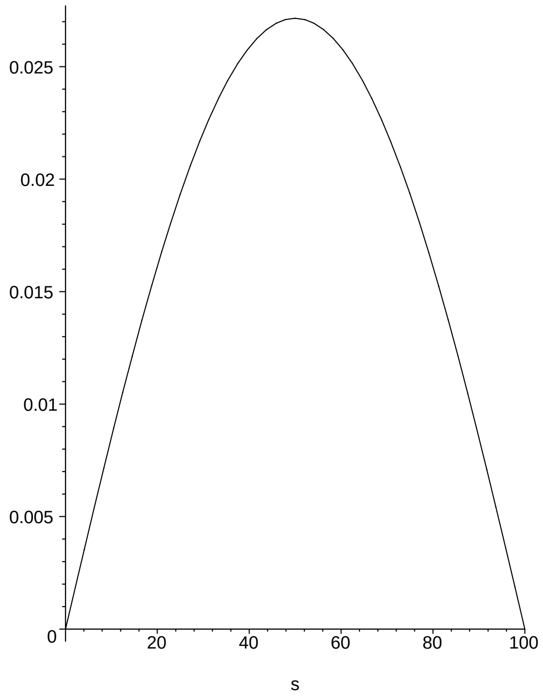

Fig. 7. Deflection of a catenary with case (a) boundary conditions. The scaled displacement $(10^{-6}ac_{33}/(\pi a^2 z_0 W_0))u_x$ is plotted as a function of $s = z/a$.

at the ends $z = 0$ and $z = z_0$. In this case the cable develops an out-of-plane bend with simple bending and flexure occurring in both the (x, z) and (y, z) planes. The scaled displacement field is shown on Fig. 8. The load is supported at the ends by resultant forces in the (x, z)-plane. The corresponding $\cos\theta$ and $\sin\theta$ components of the stress field at $z = 0$ are shown on Figs. 9 and 10.

6. Composite cylinders

Jolicoeur and Cardou (1994) have considered the simple bending of a composite hollow cable. The inner cylindrical shell consists of a uniform transversely isotropic material which is helically wound about the cylinder axis with a helical angle of 15°. The material constants for this material have been used in the earlier sections of this paper. A second cylindrical shell, consisting of another uniform transversely isotropic material, is helically wound about the first with a helical angle of −25°, so the system is contrawound. The cases where the layers are either bonded together or make a frictionless contact are considered. Jolicoeur and Cardou solve the problem by using a Lekhnitskii stress function approach, and find the bending stiffness and the stress fields for simple bending of this composite cylinder. The approach described in this paper has been used by Crossley (2002) to tackle such bending and flexure problems. The eigenvectors described in Section 2, which correspond to the positive and zero eigenvalues of the matrix $\boldsymbol{M}(q)$ in (2.8), must be supplemented by the eigenvectors corresponding to the negative eigenvalues q_4 and q_5 from (2.13). These generate stress and displacement fields which are singular on the axis $r = 0$ of the cylinder, but provide sufficient generality to enable the boundary conditions on the inside of a hollow cylinder or the

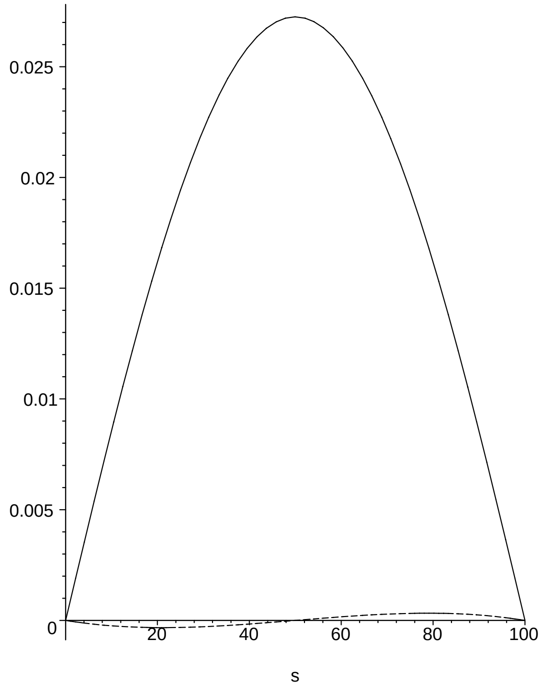

Fig. 8. Deflection of a catenary with case (b) boundary conditions. The scaled displacement components $(10^{-6}ac_{33}/(\pi a^2 W_0 z_0))(u_x, u_y)$ are plotted as functions of $s = z/a$.

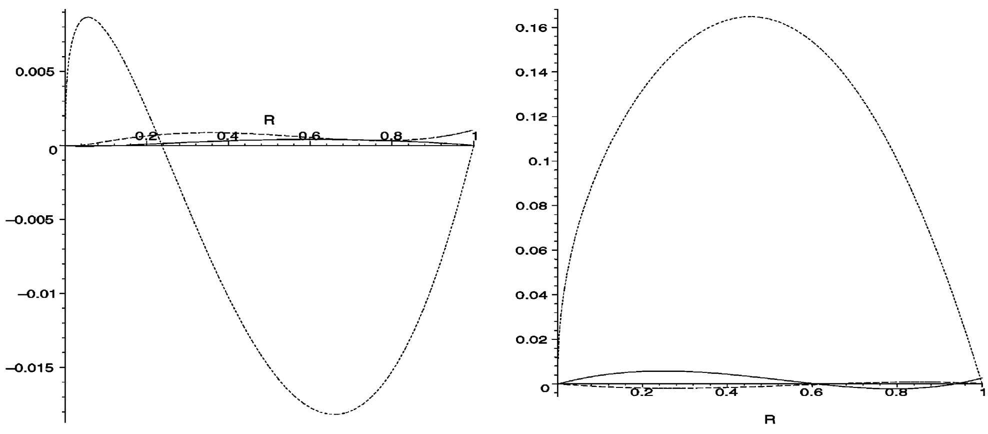

(a) $\sigma_{rr}, \sigma_{r\theta}, \sigma_{\theta\theta}$ (b) $\sigma_{zz}, \sigma_{rz}, \sigma_{\theta z}$

Fig. 9. Deflection of a catenary of length $z_0 = 100a$ by a body force W_0. The $\cos\theta$ components of the non-dimensional stress field on $z = 0$ are plotted as a function of $R = r/a$.

contact conditions between the cylindrical layers to be satisfied. Details are omitted here but may be found in Crossley (2002).

As a test of the analysis presented in this paper, the problem considered by Jolicoeur and Cardou (1994) was solved. They apply the bending moment $M_X = 10$ N m to the composite cable which causes its axis to

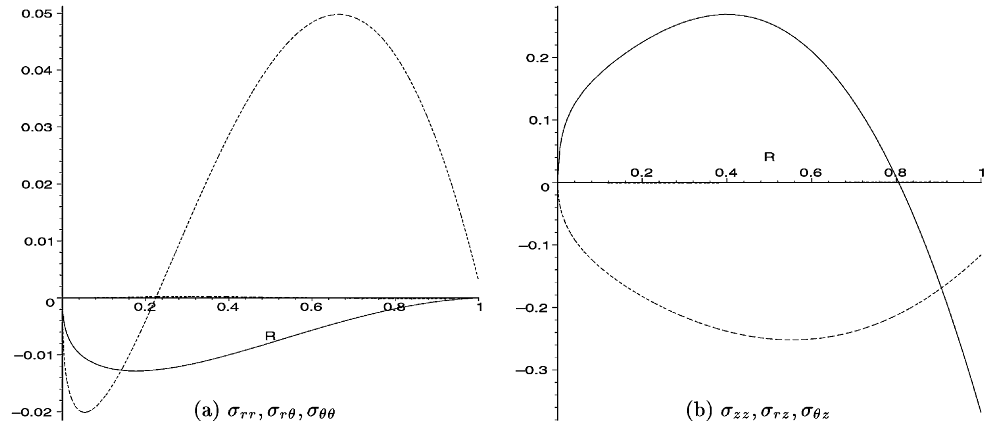

Fig. 10. Deflection of a catenary of length $z_0 = 100a$ by a body force W_0. The $\sin\theta$ components of the non-dimensional stress field on $z = 0$ are plotted as a function of $R = r/a$.

deform into the shape $u_y = -(1/2)Cz^2$ in the (y, z)-plane. The internal and external cylindrical surfaces are assumed to be traction-free and the interface either bonded or making a frictionless contact. The results we have obtained are displayed on Fig. 11 which corresponds to the results presented by Jolicoeur and Cardou. The bending stiffness of 707.73245 N m^2 for the bonded case and 498.47619 N m^2 for the frictionless case agree with the results of Jolicoeur and Cardou to three decimal places, so that the curvature C has the value 10/707.73 m^{-1} in the bonded case and 10/498.48 m^{-1} in the frictionless case.

The graphical results of Fig. 11 are almost in exact agreement with those of Jolicoeur and Cardou, except that we should note that we have used metres and N/m^2 as units for consistency with the rest of this paper. The solid lines correspond to the bonded case and the dotted lines to the frictionless case. Note that the behaviour is quite different in the two cases. When there is bonding between the layers only the stress components $\sigma_{\theta\theta}$, $\sigma_{\theta z}$ and σ_{zz} are discontinuous across the interface and the normal stress σ_{rr} is compressive on $\theta = \pi/2$ and tensile on $\theta = -\pi/2$. In the case of frictionless conditions the tangential displacement u_θ and, in particular, the axial displacement u_z have sharp discontinuities across the interface. The largest discontinuity is in the axial displacement and it has its maximum value on the neutral ($y = 0$) plane. The radial stress σ_{rr} drops to zero at the interface (this may be proved analytically) and the stress components σ_{zz}, $\sigma_{\theta\theta}$ and $\sigma_{\theta z}$ have discontinuities across the interface. This raises the possibility that differential slip, both axially and tangentially, may be more likely to occur under frictionless conditions. Also, from a practical point of view, since the frictionless and bonded solutions are so different, good predictions of the state of stress in a composite cable can only be made when the interface conditions are known and modelled accurately.

Further investigations of composite cables under simple bending, flexure and more general loading conditions have been examined by Crossley (2002).

7. One-dimensional model

The behaviour of this helically wound cable may be modelled using a one-dimensional theory relating the bending of the axis of the cylinder with the shear forces and bending moments at each cross-section. For an initially straight cable with the applied transverse loads $F_X(z)\boldsymbol{i} + F_Y(z)\boldsymbol{j}$ per unit length, the equilibrium equations are

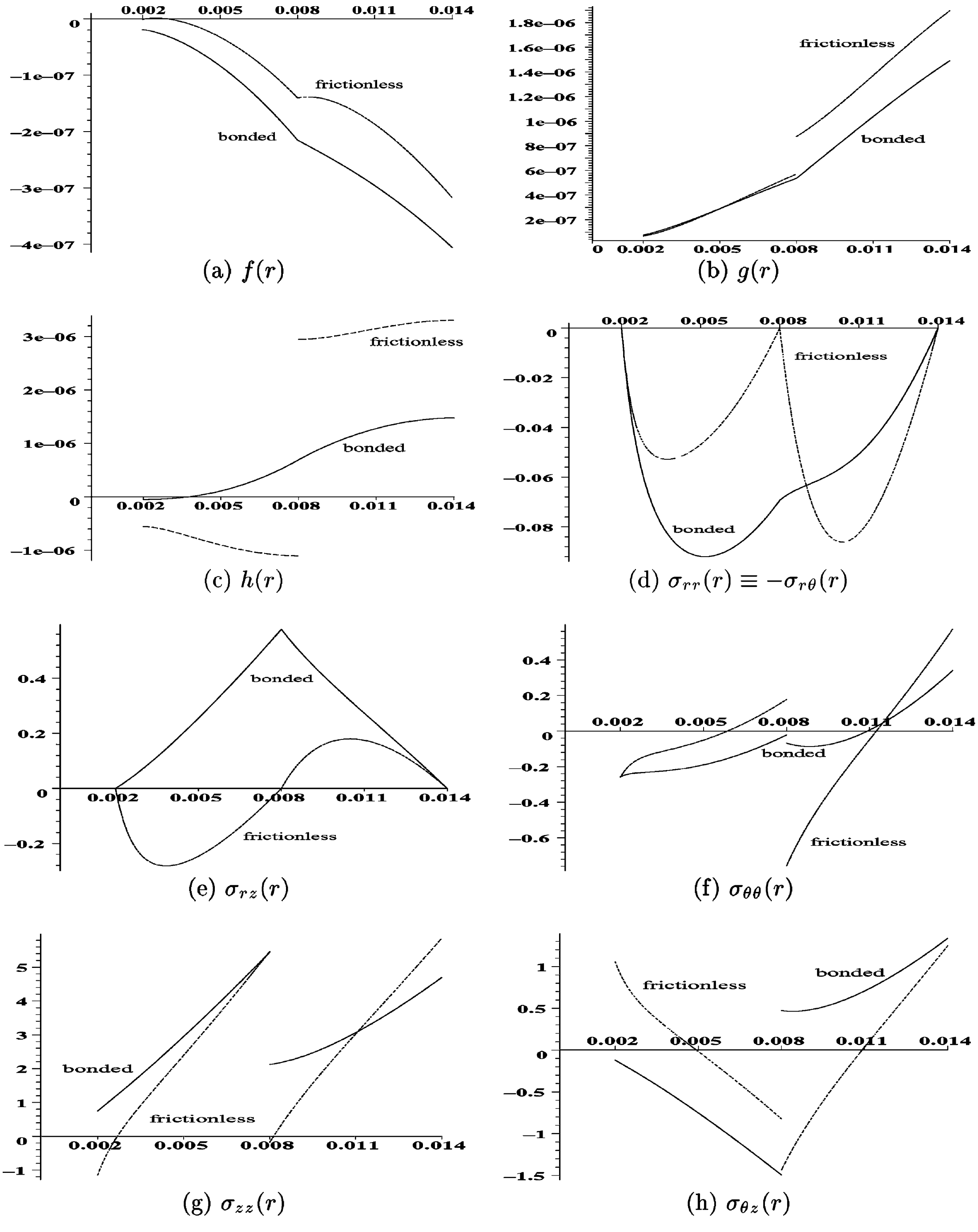

Fig. 11. Graphs of displacements in the simple bending case for a two layered hollow cable with constants from Jolicoeur and Cardou (1994), for both bonded and frictionless conditions: (a) graph of $f(r)$, where $u_r = f(r)\sin\theta - (1/2)Cz^2\sin\theta$, (b) graph of $g(r)$, where $u_\theta = g(r)\cos\theta - (1/2)Cz^2\cos\theta$, and (c) graph of $h(r)$, where $u_z = h(r)\cos\theta + Crz\sin\theta$. The remainder are graphs of the stress field $\sigma_{ij}(r)$ as stated against radial distance, r, in the simple bending case.

$$X'(z) = -F_X(z), \quad Y'(z) = -F_Y(z),$$
$$M'_X(z) = Y(z), \quad M'_Y(z) = -X(z). \tag{7.1}$$

The constitutive relations for a helically wound cylinder of this type relate the curvature to the bending moments and shear forces and have the form

$$b_s u_{x,zz} = M_Y(z) - \alpha Y(z), \tag{7.2}$$

$$b_s u_{y,zz} = -M_X(z) + \alpha X(z), \tag{7.3}$$

where b_s is the bending stiffness of the cable and α is a constant for the cable. In vector form this becomes

$$b_s \boldsymbol{D}_{,zz} = -\boldsymbol{k} \times (\boldsymbol{M} - \alpha \boldsymbol{S}), \tag{7.4}$$

where $\boldsymbol{D}$ is the transverse displacement of the axis of the cable, $\boldsymbol{M}$ the bending moment and $\boldsymbol{S}$ the shear force in the cable. This model may be used to give a physical interpretation to some of the constants occurring in the previous sections of the work which were generated directly from some Maple manipulations.

7.1. Simple bending

The solution obtained in Section 3 with a constant value M_Y^0 for $M_Y(z)$ and $X = 0$, $Y = 0$, $M_X = 0$, yields

$$u_{x,zz} = M_Y^0/b_s, \quad u_{y,zz} = 0,$$

giving a constant curvature in the (x, z)-plane. The bending stiffness for Jolicoeur and Cardou's constants (3.9) has the value of b_s given in (3.13) as

$$b_s = 23.154a^4 \times 10^9 \text{ N m}^2. \tag{7.5}$$

7.2. Flexure

The solutions obtained in Section 4 first found the resultant forces and moments necessary to maintain the displacement field $u_x = (1/6)Dz^3$ and $u_y = 0$. The resultant forces (4.13) are $X = -b_s D$, $Y = 0$, $M_X = -45.035a^5 D \times 10^9$, $M_Y = Db_s z$. If these are substituted into the constitutive relations (7.2) and (7.3), the curvature relation (7.2) is satisfied exactly and (7.3) reduces to

$$0 = -M_X + \alpha X.$$

Hence, using Jolicoeur and Cardou's constants (3.9), the material constant α has the value

$$\alpha = 1.945a. \tag{7.6}$$

The second solution obtained in Section 4 corresponds to the cantilever problem with an end load X_0. The shear force and bending moments are given by (4.14) and the only non-zero terms are $X = X_0$, $M_Y = X_0(z_0 - z)$. The corresponding curvatures are

$$b_s u_{x,zz} = X_0(z_0 - z), \quad b_s u_{y,zz} = \alpha X_0. \tag{7.7}$$

If these are integrated subject to the built-in boundary conditions

$$u_x(0) = 0, \quad u_{x,z}(0) = 0, \quad u_y(0) = 0, \quad u_{y,z}(0) = 0, \tag{7.8}$$

the displacements (4.15) are found and the numerical multipliers 7.198×10^{-12} and 4.20×10^{-11} can be identified as $(6b_s)^{-1}$ and $\alpha/(2b_s)$.

7.3. Body force solutions

The first solution corresponds to the deformation $u_x = Ez^4/24$, $u_y = 0$. This was maintained by the resultant force and moment field (5.3), namely

$$X = -\pi a^2 W_0 z, \quad Y = -6.110a^3 W_0, \quad M_X = -6.110a^3 z W_0, \quad M_Y = \tfrac{1}{2}\pi a^2 z^2 W_0 - 2.738a^4 W_0. \tag{7.9}$$

If the expression for M_Y is scaled in terms of the overall length z_0 of the cable it becomes

$$M_Y = \frac{1}{2}\pi a^2 W_0 z_0^2\left(\left(\frac{z}{z_0}\right)^2 - 1.447\left(\frac{a}{z_0}\right)^2\right). \tag{7.10}$$

The quantity z_0/a is the scaled natural length of the cylinder which must be large for this Saint-Venant theory to be relevant. The second term in (7.10) is small compared with the first term except near to the built-in end of the cable where we might expect these solutions to be least accurate. So, for the purpose of constructing a one-dimensional theory, we shall suppose that this term could be adjusted by a quantity proportional to $(a/z_0)^2$. We postulate

$$M_Y = \frac{1}{2}\pi a^2 W_0 z_0^2\left(\left(\frac{z}{z_0}\right)^2 - k\left(\frac{a}{z_0}\right)^2\right), \tag{7.11}$$

where k is a constant to replace the last term in (7.9). This is equivalent to supposing that the boundary conditions which hold on the end face $z = 0$ of the cable whose centre line satisfies the constitutive relations (7.2) and (7.3) differ by a term of order $(a/z_0)^2$ from those which are applied over the end face $z = 0$ of the cable in Section 5.

Using (7.2) and (7.3), these relations reduce to

$$\tfrac{1}{2}b_s E z^2 = \tfrac{1}{2}\pi a^2 z^2 W_0 - \tfrac{1}{2}\pi k a^4 W_0 + \alpha 6.110 a^3 W_0 \tag{7.12}$$

and

$$0 = 6.110a^3 W_0 z + \alpha(-\pi a^2 W_0 z), \tag{7.13}$$

so that, from (7.13), the numerical value of 6.110 is seen to be

$$6.110 = \alpha\pi/a. \tag{7.14}$$

Eq. (7.12) now implies

$$E = \pi a^2 W_0/b_s, \qquad k = 6.110\alpha\frac{2}{\pi a} = 7.56, \tag{7.15}$$

after some manipulation. The value of E found in (5.2) has precisely the value given in (7.15).

The second solution of Section 5 corresponds to the cantilever problem with the force field $F_X(z)$ equal to $\pi a^2 W_0$ and the end-face unstressed. The resultant forces and moments are given in (5.5) with the non-zero terms

$$X = \pi a^2 W_0(z_0 - z), \qquad M_Y = \tfrac{1}{2}\pi a^2 W_0(z - z_0)^2. \tag{7.16}$$

The constitutive relations define the curvatures

$$b_s u_{x,zz} = \tfrac{1}{2}\pi a^2 W_0(z - z_0)^2, \qquad b_s u_{y,zz} = \alpha\pi a^2 W_0(z_0 - z). \tag{7.17}$$

On integrating these equations subject to the built-in conditions (7.8) at $z = 0$ we find

$$
\begin{aligned}
b_s u_x &= \left(\frac{1}{24}\right)\pi a^2 W_0 z^2 (z^2 - 4 z z_0 + 6 z_0^2), \\
b_s u_y &= (\alpha/6)\pi a^2 W_0 z^2 (3 z_0 - z).
\end{aligned}
\tag{7.18}
$$

The numerical coefficients in (5.7) can now be identified and confirmed, but it should be noted that the final term in $(5.7)_1$ has the order of $(a/z_0)^2$ compared with the other terms in the expression and can be neglected except near the built-in end of the cable. Again, this term must be due to the fine structure of the boundary conditions on the end-face $z = 0$ of the cylinder which has been induced by our solution in Section 5.

7.4. Catenary problems

We need to solve the system of equations

$$
\begin{aligned}
&X'(z) = -\pi a^2 W_0, \quad Y'(z) = 0, \\
&M_X'(z) = Y(z), \quad M_Y'(z) = -X(z), \\
&b_s u_{x,zz} = M_Y(z) - \alpha Y(z), \\
&b_s u_{y,zz} = -M_X(z) + \alpha X(z),
\end{aligned}
\tag{7.19}
$$

subject to boundary conditions of the form of (5.9) (a) or (b).

In case (a), with the boundary conditions $u_x = 0$, $u_y = 0$, $u_{y,z} = 0$, $M_Y = 0$ at $z = 0$ and $z = z_0$, integration of the system yields

$$
\begin{aligned}
&X(z) = -\pi a^2 W_0 (z - z_0/2), \qquad Y(z) = -\alpha\pi a^2 W_0, \\
&M_X(z) = -\alpha\pi a^2 W_0 (z - z_0/2), \qquad M_Y(z) = \pi a^2 W_0 z (z - z_0)/2,
\end{aligned}
\tag{7.20}
$$

which agree with Eq. (5.11), and

$$
b_s u_x = \frac{\pi a^2 W_0}{24}\left(z^4 - 2z^3 z_0 + z z_0^3 + 12\alpha^2 (z^2 - z z_0)\right), \qquad b_s u_y = 0,
\tag{7.21}
$$

and we note that u_x is symmetrical about the midpoint $z = z_0/2$.

Similarly, in case (b) with the boundary conditions $u_x = 0$, $u_y = 0$, $M_X = 0$, $M_Y = 0$ at $z = 0$ and $z = z_0$, integration of the system yields

$$
\begin{aligned}
&X(z) = -\pi a^2 W_0 (z - z_0/2), \qquad Y(z) = 0, \\
&M_X(z) = 0, \qquad M_Y(z) = \pi a^2 W_0 (z^2 - z_0 z)/2,
\end{aligned}
\tag{7.22}
$$

with the displacement fields

$$
\begin{aligned}
b_s u_x &= \frac{\pi a^2 W_0}{24}(z^4 - 2z^3 z_0 + z z_0^3), \\
b_s u_y &= -\alpha \frac{\pi a^2 W_0}{12}(2z^3 - 3 z_0 z^2 + z_0^2 z),
\end{aligned}
\tag{7.23}
$$

and we note that u_x is symmetrical and u_y is antisymmetrical about the midpoint $z = z_0/2$ of the cable.

8. Discussion

The analysis presented in this paper has found exact solutions, in a Saint-Venant sense, for the bending of a helically reinforced cylinder when the transverse displacement field is a polynomial of degree four in the axial co-ordinate z. This work may be generalised in more than one direction.

The extension of the analysis to cables with two or three layers of different helically wound materials has been carried out by Crossley (2002) and is briefly reported in Section 6. In this work the cases where the layers are bonded together or make a frictionless contact are both considered. The analysis could also be extended to more layers but it is subject to an increasing algebraic complexity.

A second generalisation is to suppose the transverse displacement field is a polynomial of degree n in z. Clearly we can extend the analysis presented here by maintaining the same pattern for the highest-order coefficients in the field as that which is used in (2.6). These terms give rise to a strain field in which the only non-zero component is e_{zz} and this has degree $n-2$ in z. If the other expressions in (2.6) are also extended by using homogeneous terms of the form $zr^{q-1}, z^2r^{q-2}, \dots, z^{n-2}r^{q+2-n}$, the equilibrium equations may be formed. These will reduce to a matrix system of the structure of (2.8) with $\boldsymbol{M}(q)$ having a partitioned form, as in (2.11), but with a larger system of linear equations. For example, for a sixth-degree polynomial, the homogeneous expressions must include all powers of z up to terms of the form z^4r^{q-4} and the system of equations is of order 27×27. The form for $\boldsymbol{M}(q)$ has 3×3 matrices along the leading diagonal from $\boldsymbol{M}_{11}(q)$ to $\boldsymbol{M}_{99}(q)$, with a sparse array of matrices above the leading diagonal. These matrices will be related by expressions of the form given in (2.12) and the particular solutions and the eigenvectors can be generated as in Section 2. The boundary values of σ_{rr}, $\sigma_{r\theta}$, σ_{rz} on the cylindrical surface $r = a$ will also reduce to polynomials in z multiplying $\cos\theta$ or $\sin\theta$. Assuming the imposed surface tractions have this form, or appropriate body-force terms have been inserted into the equilibrium equations, higher-order bending solutions for the cylinder may be found. A similar approach is possible to find solutions which depend on $\cos(n\theta)$ and $\sin(n\theta)$.

Recently Martin and Berger (2002) have considered the propagation of mechanical waves along ACSR (aluminium conductor steel reinforced) power lines and given references to previous work on the vibrations of wire ropes. In general one-dimensional models are used to form the equations of motion. As we have found no coupling between the bending solutions described in this paper and the extension–torsion solutions found by Blouin and Cardou (1989), we might expect uncoupled wave phenomena to occur. The one-dimensional constitutive equation (7.4) yields a simple model for the bending of these anisotropic cylinders at points remote from their points of support. It is easily shown, on replacing Eq. (7.1) by the appropriate equations of motion, that two helical bending waves can propagate along such anisotropic cylinders. The wave speeds are ω/p_1 and ω/p_2, where p_1 and p_2 are the positive roots of the equation

$$p^4 = \left(\frac{m\omega^2}{b_s}\right)(1 \pm \alpha p), \tag{8.1}$$

where ω is the frequency, m is the mass per unit length of the cable, b_s is the bending stiffness and α the anisotropic cable constant. Further investigation of dynamic phenomena for helically reinforced cables can be based on this one-dimensional model or the full three-dimensional system.

Acknowledgements

The authors gratefully acknowledge the award of a CASE studentship to J.A. Crossley from British Energy Generation Limited and the Engineering and Physical Sciences Research Council. The scientific support and insight provided by R.I.A. Elrick of British Energy Generation Limited has been much appreciated.

Appendix A. The stress–strain relations

The elastic constants λ, α, β, which occur in the constitutive equation (2.1), namely

$$\sigma_{ij} = \lambda e_{kk}\delta_{ij} + 2\mu_{\mathrm{T}} e_{ij} + \alpha(a_k a_\ell e_{k\ell}\delta_{ij} + a_i a_j e_{kk}) + 2(\mu_{\mathrm{L}} - \mu)(a_i a_k e_{kj} + a_j a_k e_{ki}) + \beta a_i a_j a_k a_\ell e_{kl}, \tag{A.1}$$

may be expressed directly in terms of the extension moduli E_{L} and E_{T} for uniaxial tension along and orthogonal to the direction $\boldsymbol{a}$, the Poisson's ratios ν_{L} and ν_{T} associated with these extensions and μ_{L} and μ_{T} which are the shear moduli along and orthogonal to the direction $\boldsymbol{a}$. Using the notation of Blouin and Cardou (1989), these reduce to

$$\begin{aligned}
&\mu_{\mathrm{T}} = E_{\mathrm{T}}/[2(1+\nu_{\mathrm{T}})],\\
&\lambda = E_{\mathrm{T}}\left(\frac{E_{\mathrm{T}}\nu_{\mathrm{T}}}{E_{\mathrm{L}}} + \nu_{\mathrm{L}}^2\right)\Big/(1+\nu_{\mathrm{T}})\gamma,\\
&\alpha = E_{\mathrm{T}}\left[\nu_{\mathrm{L}}(1+\nu_{\mathrm{T}}-\nu_{\mathrm{L}})\frac{E_{\mathrm{T}}\nu_{\mathrm{T}}}{E_{\mathrm{L}}}\right]\Big/(1+\nu_{\mathrm{T}})\gamma,\\
&\beta = E_{\mathrm{T}}(1-\nu_{\mathrm{T}})/\gamma - 4\mu_{\mathrm{L}} + 2\mu_{\mathrm{T}} - 2\alpha - \lambda,
\end{aligned} \tag{A.2}$$

where

$$\gamma = (1-\nu_{\mathrm{T}})E_{\mathrm{T}}/E_{\mathrm{L}} - 2\nu_{\mathrm{L}}^2. \tag{A.3}$$

Note that a uniaxial stress in the T-direction (orthogonal to $\boldsymbol{a}$) generates a strain with Poisson's ratio ν_{L} in the L-direction, and a strain with Poisson's ratio ν_{T} in an orthogonal T-direction. In addition, ν_{L}' strain in the T-direction due to a uniaxial stress in the L-direction and that these are connected by the relation

$$E_{\mathrm{T}}\nu_{\mathrm{L}}' = E_{\mathrm{L}}\nu_{\mathrm{L}}. \tag{A.4}$$

Note also that there are only five independent elastic constants.

When the constitutive equation is put into cylindrical polar co-ordinates (r, θ, z) and the principal direction of transverse isotropy is taken along the helical direction

$$\boldsymbol{a} = \boldsymbol{e}_\theta \sin\delta + \boldsymbol{e}_z \cos\delta, \tag{A.5}$$

where δ is the lay angle of the helical strands, the elastic stiffness matrix defined in (2.3) has the form

$$\begin{aligned}
&c_{11} = \lambda + 2\mu_{\mathrm{T}},\ \ c_{12} = \lambda + \alpha\sin^2\delta,\ \ c_{13} = \lambda + \alpha\cos^2\delta,\ \ c_{14} = \alpha\sin\delta\cos\delta,\\
&c_{22} = \lambda + 2\mu_{\mathrm{T}}\cos 2\delta + (4\mu_{\mathrm{L}} + 2\alpha + \beta\sin^2\delta)\sin^2\delta,\ \ c_{23} = \lambda + \alpha + \beta\sin^2\delta\cos^2\delta,\\
&c_{24} = (\alpha + 2\mu_{\mathrm{L}} - 2\mu_{\mathrm{T}} + \beta\sin^2\delta)\sin\delta\cos\delta,\\
&c_{33} = \lambda - 2\mu_{\mathrm{T}}\cos 2\delta + (4\mu_{\mathrm{L}} + 2\alpha + \beta\cos^2\delta)\cos^2\delta,\\
&c_{34} = (\alpha + 2\mu_{\mathrm{L}} - 2\mu_{\mathrm{T}} + \beta\cos^2\delta)\sin\delta\cos\delta,\ \ c_{44} = \mu_{\mathrm{L}} + \beta\sin^2\delta\cos^2\delta,\\
&c_{55} = \mu_{\mathrm{T}}\sin^2\delta + \mu_{\mathrm{L}}\cos^2\delta,\ \ c_{56} = (\mu_{\mathrm{L}} - \mu_{\mathrm{T}})\cos\delta\sin\delta,\ \ c_{66} = \mu_{\mathrm{T}}\cos^2\delta + \mu_{\mathrm{L}}\sin^2\delta.
\end{aligned} \tag{A.6}$$

Appendix B. The submatrices of $\boldsymbol{M}(\boldsymbol{q})$

In Eq. (2.11) the 15×15 matrix $\boldsymbol{M}(q)$ is partitioned into a set of 3×3 submatrices which are detailed below. The matrices are closely related to each other.

$$\boldsymbol{M}_{11}(q) = \begin{pmatrix} c_{11}q^2 - c_{22} - c_{66} & (c_{12}+c_{66})q - c_{22} - c_{66} & (c_{14}+c_{56})q - c_{24} \\ -(c_{12}+c_{66})q - c_{22} - c_{66} & c_{66}q^2 - c_{22} - c_{66} & c_{56}(q^2+q) - c_{24} \\ -(c_{14}+c_{56})q - c_{24} & c_{56}(q^2-q) - c_{24} & c_{55}q^2 - c_{44} \end{pmatrix},$$

$$\boldsymbol{M}_{22}(q) = \begin{pmatrix} c_{11}q^2 - c_{22} - c_{66} & -(c_{12}+c_{66})q + c_{22} + c_{66} & -(c_{14}+c_{56})q + c_{24} \\ (c_{12}+c_{66})q + c_{22} + c_{66} & c_{66}q^2 - c_{22} - c_{66} & c_{56}(q^2+q) - c_{24} \\ (c_{14}+c_{56})q + c_{24} & c_{56}(q^2-q) - c_{24} & c_{55}q^2 - c_{44} \end{pmatrix},$$

$$\boldsymbol{M}_{33}(q) = \boldsymbol{M}_{11}(q-1), \quad \boldsymbol{M}_{44}(q) = \boldsymbol{M}_{22}(q-1), \quad \boldsymbol{M}_{55}(q) = \boldsymbol{M}_{11}(q-2),$$

$$\boldsymbol{M}_{14}(q) = \begin{pmatrix} 2c_{56} & (c_{14}+c_{56})q - c_{24} - 2c_{56} & (c_{13}+c_{55})q - c_{23} - c_{55} \\ (c_{14}+c_{56})q + c_{24} + c_{56} - c_{14} & -2c_{24} & -c_{44} - c_{23} \\ (c_{13}+c_{55})q - c_{13} + c_{23} & -c_{23} - c_{44} & -2c_{34} \end{pmatrix},$$

$$\boldsymbol{M}_{15}(q) = \begin{pmatrix} c_{55} & 0 & 0 \\ 0 & c_{44} & c_{34} \\ 0 & c_{34} & c_{33} \end{pmatrix},$$

$$\boldsymbol{M}_{23}(q) = \begin{pmatrix} -2c_{56} & (c_{14}+c_{56})q - c_{24} - 2c_{56} & (c_{13}+c_{55})q - c_{23} - c_{55} \\ (c_{14}+c_{56})q + c_{24} + c_{56} - c_{14} & 2c_{24} & c_{23} + c_{44} \\ (c_{13}+c_{55})q - c_{13} + c_{23} & c_{23} + c_{44} & 2c_{34} \end{pmatrix},$$

$$\boldsymbol{M}_{45}(q) = \boldsymbol{M}_{23}(q-1).$$

References

Blouin, F., Cardou, A., 1989. A study of helically reinforced cylinders under symmetric loads and application to strand mathematical modelling. Int. J. Solids Struct. 25 (2), 189–200.

Cardou, A., Jolicoeur, C., 1997. Mechanical models of helical strands. Appl. Mech. Rev. 50, 1–14.

Crossley, J.A., 2002. Ph.D. Thesis, University of Nottingham.

Costello, G.A., 1978. Analytical investigation of wire rope. Appl. Mech. Rev. 31, 897–900.

Costello, G.A., 1997. Theory of Wire Rope, second ed. Springer, Berlin.

Jolicoeur, C., Cardou, A., 1994. Analytical solution for bending of coaxial orthotropic cylinders. ASCE J. Eng. Mech. 120 (12), 2556–2574.

Jolicoeur, C., Cardou, A., 1996. Semi-continuous mathematical model for bending of multilayered wire strands. ASCE J. Eng. Mech. 122 (7), 643–650.

Lanteigne, J., 1985. Theoretical estimation of the response of helically armored cables to tension, torsion and bending. J. Appl. Mech. 52, 423–432.

Lekhnitskii, S.G., 1981. Theory of Elasticity of an Anisotropic Body. Mir Publishers, Moscow.

Martin, P.A., Berger, J.R., 2002. On mechanical waves along ACSR electrical power lines. ASME J. Appl. Mech. 69, 740–748.

Raoof, M., Kraincanic, I., 1994. Critical examination of various approaches used for analysing helical cables. J. Strain Anal. 29 (1), 43–55.

Spencer, A.J.M. (Ed.), 1984. Continuum Theory of the Mechanics of Fibre-Reinforced Composites, CISM notes 282. Springer, Wien, New York.

Utting, W.S., Jones, N., 1984. Survey of literature on the behaviour of wire ropes. Wire Ind., 623–629.

Utting, W.S., 1994. Survey of the literature on the behaviour of steel wire ropes: Part I. Wire Ind., 633–635, Part II. Wire Ind., 1994, 746–748; Part III. Wire Ind., 1995, 269–279.